

The anti-Jaynes-Cummings model is solvable : quantum Rabi model in rotating and counter-rotating frames ; following the experiments

Joseph Omolo (✉ ojakeyo@maseno.ac.ke)

MASENO UNIVERSITY <https://orcid.org/0000-0002-8950-2095>

Article

Keywords: anti-Jaynes-Cummings model, quantum Rabi model, rotating frame

Posted Date: April 8th, 2021

DOI: <https://doi.org/10.21203/rs.3.rs-379917/v1>

License:  This work is licensed under a Creative Commons Attribution 4.0 International License.

[Read Full License](#)

The antiJaynes-Cummings model is solvable : quantum Rabi model in rotating and counter-rotating frames ; following the experiments

Joseph Akeyo Omolo

Department of Physics, Maseno University, P.O. Private Bag, Maseno, Kenya
e-mail: ojakeyo04@yahoo.co.uk ; ojakeyo@maseno.ac.ke

20 February 2021

Abstract

This article is a response to the continued assumption, cited even in reports and reviews of recent experimental breakthroughs and advances in theoretical methods, that the antiJaynes-Cummings (AJC) interaction is an intractable energy non-conserving component of the quantum Rabi model (QRM). We present three key features of QRM dynamics : (a) the AJC interaction component has a conserved excitation number operator and is exactly solvable (b) QRM dynamical space consists of a rotating frame (RF) dominated by an exactly solved Jaynes-Cummings (JC) interaction specified by a conserved JC excitation number operator which generates the $U(1)$ symmetry of RF and a correlated counter-rotating frame (CRF) dominated by an exactly solved antiJaynes-Cummings (AJC) interaction specified by a conserved AJC excitation number operator which generates the $U(1)$ symmetry of CRF (c) for QRM dynamical evolution in RF, the initial atom-field state $|e0\rangle$ is an eigenstate of the effective AJC Hamiltonian \bar{H}_{AJC} , while the effective JC Hamiltonian H_{JC} drives this initial state $|e0\rangle$ into a time evolving entangled state, and, in a corresponding process for QRM dynamical evolution in CRF, the initial atom-field state $|g0\rangle$ is an eigenstate of the effective JC Hamiltonian, while the effective AJC Hamiltonian drives this initial state $|g0\rangle$ into a time evolving entangled state, thus addressing one of the long-standing challenges of theoretical and experimental QRM dynamics; consistent generalizations of the initial states $|e0\rangle$, $|g0\rangle$ to corresponding $n \geq 0$ entangled eigenstates $|\bar{\Psi}_{en}^+\rangle$, $|\Psi_{gn}^-\rangle$ of the AJC in RF and JC in CRF, respectively, provides general dynamical evolution of QRM characterized by collapses and revivals in the time evolution of the atomic, field mode, JC and AJC excitation numbers for large initial photon numbers ; the JC and AJC excitation numbers are conserved in the respective frames RF, CRF, but each evolves with time in the alternate frame.

1 Introduction

The quantum Rabi model (QRM) is the simplest form of quantized light-matter interaction coupling a single two-level atom to a single mode of quantized light. The Hamiltonian of the system takes the standard form

$$H_R = \hbar\omega \left(\hat{a}^\dagger \hat{a} + \frac{1}{2} \right) + \hbar\omega_0 s_z + \hbar g (\hat{a} + \hat{a}^\dagger) (s_- + s_+) ; \quad s_z = \frac{1}{2} \sigma_z ; \quad \sigma_x = s_- + s_+ \quad (1)$$

where $(\hat{a}, \hat{a}^\dagger, \omega)$ and $(s_z, s_-, s_+, \omega_0)$ are the respective quantized field mode and atomic spin state operators and frequencies with standard meanings, while g is the coupling constant. Opening the brackets in the interaction term reveals that the Hamiltonian H_R is composed of a rotating component, the Jaynes-Cummings (JC) interaction and a counter-rotating component, the antiJaynes-Cummings (AJC) interaction, which we obtain explicitly below. Since the two components are algebraically correlated in the sense that they do not commute, the quantum Rabi Hamiltonian H_R must be considered in its full form, which has made it too difficult, if not impossible, to determine the exact general time evolving state of QRM.

Great advances have been made in developing fairly accurate theoretical methods [1-5] to gain insight into QRM dynamics beyond the rotating wave approximation (RWA). However, a major drawback has remained the long-standing assumption that the antiJaynes-Cummings component does not have a conserved excitation number and is not exactly solvable, even though it is now several years since the present author constructed the AJC excitation number operator and proved its conservation in [6], followed by simpler reformulation

39 and exact solutions of both JC and AJC dynamics in [7 , 8]. The good news is that experiments on the
40 full QRM have now made outstanding breakthroughs, determining details of the dynamics someway into the
41 USC-DSC regimes [9-12]. However, in both theoretical and experimental advances, the lack of information
42 on the solvability of the AJC interaction has meant that the coupling range is defined only from the JC
43 side where the rotating wave approximation (RWA) applies, considering the USC-DSC regimes far beyond
44 the RWA as the dynamical region dominated by the counter-rotating component of QRM. Since the main
45 purpose of the present article is to supply the long-missing information on the conserved excitation number
46 operator and exact solutions of the AJC interaction, we do not give details of the general historical and
47 technical developments of the outstanding theoretical and experimental achievements made so far on QRM,
48 but refer the interested readers to the most recent excellent reviews [13 , 14 , 15].

49 This article is organized as follows : we present the basic algebraic and dynamical structure of QRM in
50 section 2, where the JC and AJC components are defined together with the respective conserved excitation
51 number, $U(1)$ and parity operators, as well as the rotating and counter-rotating frames RF , CRF, leading to
52 the corresponding rotating and counter-rotating wave approximations RWA , CRWA ; we develop dynamics
53 in RF (RWA) and CRF (CRWA) in section 3, where we provide consistent generalizations of the initial states
54 $|e0\rangle$, $|g0\rangle$ to the corresponding $n \geq 0$ entangled eigenstates of the AJC and JC in RF , CRF, respectively ;
55 the Conclusion is given in section 4.

56 2 Basic algebraic and dynamical structure of QRM

57 An important point to note is that the algebraic properties of the basic state operators of a fully quan-
58 tized system such as QRM directly determine the dynamical structure of the system. To achieve a clear
59 understanding of the internal structure of QRM dynamics, we begin by applying the algebraic properties of
60 the atom-field state operators \hat{a} , \hat{a}^\dagger , s_z , s_- , s_+ to develop the basic algebraic structure, automatically
61 leading us to identification of two algebraically correlated dynamical frames of QRM as we now present in
62 this section.

63 2.1 Basic algebraic structure of QRM

Following the original work in [6] where details are presented, we apply normal and antinormal operator
ordering of the basic atomic and quantized field mode state operators to express the standard quantum Rabi
model (QRM) Hamiltonian H_R in equation (1) in the symmetrized rotating and counter-rotating component
form [6-8]

$$H_R = \frac{1}{2}(H + \bar{H}) \quad (2a)$$

The rotating component H is the Jaynes-Cummings (JC) Hamiltonian obtained in the normal order form

$$H = \hbar\omega\hat{N} + \hbar\delta s_z + 2\hbar g(\hat{a}s_+ + \hat{a}^\dagger s_-) - \frac{1}{2}\hbar\omega \quad ; \quad \hat{N} = \hat{a}^\dagger\hat{a} + s_+s_- \quad ; \quad \delta = \omega_0 - \omega \quad (2b)$$

where \hat{N} is the standard conserved excitation number operator of the JC interaction, commuting with the
Hamiltonian H according to

$$[\hat{N} , H] = 0 \quad (2c)$$

64 which we have proved explicitly in [6-8] and is easily proved here using the JC qubit state transition operator
65 introduced in equation (5c). The parameter $\delta = \omega_0 - \omega$ in equation (2b) is the usual JC red-sideband
66 frequency detuning.

The counter-rotating component \bar{H} is the antiJaynes-Cummings (AJC) Hamiltonian obtained in the
antinormal order form

$$\bar{H} = \hbar\omega\hat{\bar{N}} + \hbar\bar{\delta}s_z + 2\hbar g(\hat{a}s_- + \hat{a}^\dagger s_+) - \frac{1}{2}\hbar\omega \quad ; \quad \hat{\bar{N}} = \hat{a}\hat{a}^\dagger + s_-s_+ \quad ; \quad \bar{\delta} = \omega_0 + \omega \quad (2d)$$

where $\hat{\bar{N}}$ is the (long-missing) conserved excitation number operator of the AJC interaction, which we first
constructed and proved conserved in [6], commuting with the Hamiltonian \bar{H} according to

$$[\hat{\bar{N}} , \bar{H}] = 0 \quad (2e)$$

67 This commutation relation is easily proved here using the AJC qubit state transition operator introduced
 68 in equation (7b) below. The parameter $\bar{\delta} = \omega_0 + \omega$ in equation (2d) is the AJC blue-sideband frequency
 69 detuning.

The JC and AJC excitation number operators \hat{N} , $\hat{\bar{N}}$ commute, but each does not commute with the alternate Hamiltonian according to

$$[\hat{N}, \hat{\bar{N}}] = 0; \quad [\hat{N}, \bar{H}] \neq 0; \quad [\hat{\bar{N}}, H] \neq 0; \quad [H, \bar{H}] \neq 0 \quad (2f)$$

70 where the last commutation relation shows that the JC and AJC components do not commute and are
 71 therefore algebraically correlated as stated earlier.

72 With the specification of the basic algebraic structure provided above, we now present the $U(1)$ and parity
 73 symmetry properties of QRM generated by the JC and AJC excitation number operators \hat{N} , $\hat{\bar{N}}$.

74 2.2 QRM in the rotating frame : RF

The free evolution operator $U_0(t) = e^{-i\omega t \hat{N}}$ generated by the JC excitation number operator \hat{N} is a $U(1)$ symmetry operator which effects transformation of the JC and AJC Hamiltonians in equations (2b), (2d) to the rotating frame (RF) according to [6]

$$U_0(t) = e^{-i\omega t \hat{N}} : \quad U_0^\dagger(t) H U_0(t) = H; \quad U_0^\dagger(t) \bar{H} U_0(t) = \hbar\omega \left(\frac{\hat{\bar{N}}}{2} - \frac{1}{2} \right) + \hbar\bar{\delta}s_z + 2\hbar g(e^{-2i\omega t} \hat{a}s_- + e^{2i\omega t} \hat{a}^\dagger s_+) \quad (3a)$$

Using equations (2a), (2b), (3a), we obtain the transformation of the QRM Hamiltonian H_R to the rotating frame reorganized in the final form

$$U_0^\dagger(t) H_R U_0(t) = H_{JC} + \hbar g(e^{-2i\omega t} \hat{a}s_- + e^{2i\omega t} \hat{a}^\dagger s_+) \quad ; \quad H_{JC} = \hbar\omega \hat{N} + \hbar\delta s_z + \hbar g(\hat{a}s_+ + \hat{a}^\dagger s_-) \quad (3b)$$

75 where H_{JC} is the effective JC Hamiltonian in the rotating frame.

According to equation (3b), the effective JC Hamiltonian H_{JC} dominates over the fast oscillating AJC interaction component in the RF. Hence, QRM dynamics in the RF is dominated by the JC interaction mechanism characterized by red-sideband transitions generated by the effective JC Hamiltonian H_{JC} . Dropping the fast oscillating AJC component in equation (3b), we obtain the QRM Hamiltonian in a rotating wave approximation (RWA) in the RF in the form

$$U_0^\dagger H_R U_0(t) \approx H_{JC} \quad (3c)$$

76 2.3 QRM in the counter-rotating frame : CRF

The free evolution operator $\bar{U}_0(t) = e^{-i\omega t \hat{\bar{N}}}$ generated by the AJC excitation number operator $\hat{\bar{N}}$ is a $U(1)$ symmetry operator which effects transformation of the JC and AJC Hamiltonians in equations (2b), (2d) to the counter-rotating frame (CRF) according to [6]

$$\bar{U}_0(t) = e^{-i\omega t \hat{\bar{N}}} : \quad \bar{U}_0^\dagger(t) \bar{H} \bar{U}_0(t) = \bar{H}; \quad \bar{U}_0^\dagger(t) H \bar{U}_0(t) = \hbar\omega \left(\hat{N} - \frac{1}{2} \right) + \hbar\delta s_z + 2\hbar g(e^{-2i\omega t} \hat{a}s_+ + e^{2i\omega t} \hat{a}^\dagger s_-) \quad (3d)$$

Using equations (2a), (2d), (3d), we obtain the transformation of the QRM Hamiltonian H_R to the counter-rotating frame reorganized in the final form

$$\bar{U}_0^\dagger(t) H_R \bar{U}_0(t) = \bar{H}_{AJC} + \hbar g(e^{-2i\omega t} \hat{a}s_+ + e^{2i\omega t} \hat{a}^\dagger s_-) \quad ; \quad \bar{H}_{AJC} = \hbar\omega \left(\hat{\bar{N}} - 1 \right) + \hbar\bar{\delta}s_z + \hbar g(\hat{a}s_- + \hat{a}^\dagger s_+) \quad (3e)$$

77 where \bar{H}_{AJC} is the effective AJC Hamiltonian in the counter-rotating frame.

According to equation (3e), the effective AJC Hamiltonian \bar{H}_{AJC} dominates over the fast oscillating JC interaction component in the CRF. Hence, QRM dynamics in the CRF is dominated by the AJC interaction mechanism characterized by blue-sideband transitions generated by the effective AJC Hamiltonian \bar{H}_{AJC} . Dropping the fast oscillating JC component in equation (3e), we obtain the QRM Hamiltonian in a counter-rotating wave approximation (CRWA) in the CRF in the form

$$\bar{U}_0^\dagger \bar{H}_R \bar{U}_0(t) \approx \bar{H}_{AJC} \quad (3f)$$

78 2.4 QRM parity symmetry

An important algebraic property has arisen that QRM is characterized by two commuting excitation number operators, namely, the JC conserved excitation number operator \hat{N} which generates $U(1)$ symmetry in the rotating frame according to equations (3a)-(3c), and the AJC conserved excitation number operator $\hat{\bar{N}}$ which generates $U(1)$ symmetry in the counter-rotating frame according to equations (3d)-(3f). The two excitation number operators commute with the respective RF/CRF Hamiltonians H_{JC} , \bar{H}_{AJC} , but each does not commute with the Hamiltonian in the alternate frame according to

$$[\hat{N}, H_{JC}] = 0; \quad [\hat{N}, \bar{H}_{AJC}] \neq 0; \quad [\hat{\bar{N}}, \bar{H}_{AJC}] = 0; \quad [\hat{\bar{N}}, H_{JC}] \neq 0; \quad [H_{JC}, \bar{H}_{AJC}] \neq 0 \quad (4a)$$

79 where we recall $[\hat{N}, \hat{\bar{N}}] = 0$ in equation (2f). We observe that equation (4a) essentially re-emphasizes the
80 commutation relations in equation (2f), now within the dynamical frames RF, CRF.

The $U(1)$ symmetry generated by either excitation number operator \hat{N} or $\hat{\bar{N}}$ in the respective frame *RF* or *CRF* is therefore not a common symmetry of the full QRM. However, in [6], we established that setting $\omega t = k\pi$, $k = 1, 2, 3, \dots$, in $U_0(t)$, $\bar{U}_0(t)$ in equations (3a), (3d), provides the parity operator $\hat{\Pi}_k = (\hat{\Pi})^k$ which generates parity symmetry as a common symmetry of QRM according to [6]

$$\hat{\Pi}_k = e^{-ik\pi\hat{N}} = e^{-ik\pi\hat{\bar{N}}} = (\hat{\Pi})^k \quad ; \quad \hat{\Pi} = e^{-i\pi\hat{N}} = e^{-i\pi\hat{\bar{N}}} \quad ; \quad k = 1, 2, 3, \dots \quad (4b)$$

$$\hat{\Pi}_k^\dagger H \hat{\Pi}_k = H \quad ; \quad \hat{\Pi}_k^\dagger \bar{H} \hat{\Pi}_k = \bar{H} \quad \Rightarrow \quad \hat{\Pi}_k^\dagger H_R \hat{\Pi}_k = H_R \quad (4c)$$

where $\hat{\Pi}$ in equation (4b) is the standard QRM parity operator in usual definition with respect to the JC excitation number operator \hat{N} , but now given equivalent definition in terms of the AJC excitation number operator $\hat{\bar{N}}$. The equality arising in the corresponding definition with respect to the AJC excitation number operator $\hat{\bar{N}}$ is easily proved [6], using the relation (recall $\hat{a}\hat{a}^\dagger = \hat{a}^\dagger\hat{a} + 1$, $s_+s_- + s_-s_+ = 1$)

$$\hat{\bar{N}} = \hat{N} + 2s_-s_+ \quad : \quad e^{-i\pi\hat{\bar{N}}} = e^{-i\pi\hat{N}} e^{-2i\pi s_-s_+} \quad ; \quad e^{-2i\pi s_-s_+} = I \quad \Rightarrow \quad e^{-i\pi\hat{\bar{N}}} = e^{-i\pi\hat{N}} = \hat{\Pi} \quad (4d)$$

81 This parity symmetry has been applied to obtain approximate solutions of QRM in the deep strong coupling
82 (DSC) regime [2] and exact stationary state solutions in [3], noting also the related dynamical evolution in
83 [1].

84 3 QRM dynamics in RF and CRF : following experiments

85 It follows from subsections 2.2 – 2.3 that QRM has two dynamical frames, namely, the rotating frame (RF)
86 and the counter-rotating frame (CRF). Dynamics in RF is dominated by the JC interaction mechanism and
87 through a $U(1)$ symmetry transformation generated by the conserved JC excitation number operator \hat{N} , the
88 QRM Hamiltonian is approximated by an effective JC Hamiltonian H_{JC} in a rotating wave approximation
89 (RWA) according to equations (3b)-(3c). Dynamics in CRF is dominated by the AJC interaction mechanism
90 and through a $U(1)$ symmetry transformation generated by the conserved AJC excitation number operator
91 $\hat{\bar{N}}$, the QRM Hamiltonian is approximated by an effective AJC Hamiltonian \bar{H}_{AJC} in a counter-rotating wave
92 approximation (CRWA) according to equations (3e)-(3f). This specification of the QRM dynamical frames
93 which we have achieved here has never been done earlier, since CRF was never known to have a conserved
94 excitation number operator, until the present author constructed the correct form $\hat{\bar{N}}$ and proved conservation
95 in [6]. By a comparison with the theoretical models [1, 2, 4, 13, 14] and experimental designs [5, 9-12, 14
96, 15] of the full QRM dynamics, RF as specified in the present article may be identified with the JC (weak-
97 strong coupling) regime, but CRF as specified here may not be interpreted as the USC-DSC regime where
98 the RWA breaks down and the counter-rotating terms (AJC interaction) start contributing to the dynamics.
99 We note that the definition of CRF in subsection 2.3 does not involve the dimensionless coupling parameter
100 $\frac{g}{\omega}$, which is explicitly used in characterizing the USC-DSC regimes [2, 4, 13, 14], meaning that CRF,
101 even though dominated by the effective AJC interaction, may not necessarily be equivalent to the USC-DSC
102 regime. The property established earlier in [6] and in the present article that QRM dynamical frames RF
103 and CRF are each specified by a corresponding conserved excitation number operator \hat{N} , $\hat{\bar{N}}$, respectively,
104 means that these commuting excitation number operators may be used as order parameters for characterizing

105 QRM dynamics in RF and CRF regions of the general quantum state space. According to the commutation
106 relations in equation (4a), the JC excitation number operator \hat{N} is conserved in the dynamics generated
107 by the effective JC Hamiltonian H_{JC} in RF, but non-conserved in the dynamics generated by the effective
108 AJC Hamiltonian \overline{H}_{AJC} in CRF, while the AJC excitation number operator \hat{N} is conserved in the dynamics
109 generated by the effective AJC Hamiltonian \overline{H}_{AJC} in CRF, but non-conserved in the dynamics generated by
110 the effective JC Hamiltonian H_{JC} in RF. The dynamical property that the JC excitation number operator
111 \hat{N} is conserved in the RF (RWA) coupling regime, but evolves with time in the USC-DSC regime has been
112 determined in QRM experiments [9]. We now follow the initial states specified in the experiments and apply
113 the RF and CRF specifications in subsections 2.2–2.3 to determine and clarify the observed physical features
114 of QRM dynamics. The experiments have focussed attention on QRM dynamics evolving from an initial state
115 with the field mode in the vacuum state and the atom in excited or ground state specified by $|e0\rangle$ or $|g0\rangle$
116 in standard notation. In the present work, we provide consistent generalizations of these atom-field initial
117 states to include field mode initial states $|n \geq 0\rangle$.

118 3.1 QRM dynamics in RF

119 We have established in subsection 2.2 that QRM dynamics in RF is generated by the effective JC Hamiltonian
120 H_{JC} in RWA according to equations (3b)-(3c). The experiments [9-12] have identified the state $|e0\rangle$ with the
121 field mode in the vacuum state $|0\rangle$ and the atom in the excited state $|e\rangle$ as the appropriate initial state for
122 QRM dynamics in RF (JC regime). Here, we establish that the initial state $|e0\rangle$ in RF is an eigenstate of the
123 effective AJC Hamiltonian \overline{H}_{AJC} and provide a consistent generalization to the corresponding $n \geq 0$ initial
124 AJC eigenstate which reduces to $|e0\rangle$ for $n = 0$.

125 3.1.1 Dynamics from initial state $|e0\rangle$

We introduce appropriate notation $|\psi_{e0}\rangle$ for the initial state and $|\psi_{g1}\rangle$ for the associated transition state
defined in standard notation as

$$|\psi_{e0}\rangle = |e0\rangle \quad ; \quad |\psi_{g1}\rangle = |g1\rangle \quad (5a)$$

We observe that the effective AJC Hamiltonian \overline{H}_{AJC} does not generate dynamical evolution of the initial
state $|e0\rangle$ in RF, since $|e0\rangle$ is an eigenstate of \overline{H}_{AJC} , which, using \overline{H}_{AJC} from equation (3e) and applying
standard atom and field mode state algebraic operations, is easily established to satisfy an eigenvalue equation
(recall $\bar{\delta} = \omega_0 + \omega$)

$$\overline{H}_{AJC}|\psi_{e0}\rangle = \frac{1}{2}\hbar(\omega_0 + \omega)|\psi_{e0}\rangle \quad (5b)$$

126 where we identify the energy eigenvalue $\frac{1}{2}\hbar(\omega_0 + \omega)$ as the atomic excited state energy $\frac{1}{2}\hbar\omega_0$ and the field
127 mode vacuum state energy $\frac{1}{2}\hbar\omega$ as expected. Equation (5b) means that the effective AJC Hamiltonian \overline{H}_{AJC}
128 generates only plane wave evolution $e^{-\frac{i\hbar}{2}(\omega_0 + \omega)t}|\psi_{e0}\rangle$ of the initial state $|\psi_{e0}\rangle$ which does not describe the
129 general QRM dynamics in RF. However, in agreement with the theoretical models and experiments, the
130 effective JC Hamiltonian H_{JC} generates dynamical evolution of the initial state $|\psi_{e0}\rangle$ into a time evolving
131 entangled state which describes the general QRM dynamics in RF as we now demonstrate.

We introduce a JC qubit state transition operator \hat{A} and apply standard algebraic properties of the atom
and field mode state operators \hat{a} , \hat{a}^\dagger , s_z , s_- , s_+ to determine the relation with the JC excitation number
operator \hat{N} in the form

$$\hat{A} = \delta s_z + g(\hat{a}s_+ + \hat{a}^\dagger s_-) \quad ; \quad \hat{A}^2 = \frac{1}{4}\delta^2 + g^2\hat{N} \quad (5c)$$

Using \hat{A} from equation (5c), we express the effective JC Hamiltonian H_{JC} defined in equation (3b) in the
form

$$H_{JC} = \hbar\omega\hat{N} + \hbar\hat{A} \quad (5d)$$

132 Conservation of the JC excitation number in the dynamics generated by H_{JC} in RF is easily proved by using
133 the relations in equations (5c), (5d) to show that \hat{N} commutes with H_{JC} , thus confirming equations (2f),
134 (4a) and simplifying the earlier proof in [6].

Applying \hat{A} from equation (5c) on the initial state $|\psi_{e0}\rangle$ defined in equation (5a), using standard atom-field
state algebraic operations and reorganizing as appropriate, we obtain JC qubit states $|\psi_{e0}\rangle$, $|\phi_{e0}\rangle$ satisfying
qubit state transition algebraic operations in the form

$$\hat{A}|\psi_{e0}\rangle = R_{e0}|\phi_{e0}\rangle \quad ; \quad \hat{A}|\phi_{e0}\rangle = R_{e0}|\psi_{e0}\rangle \quad (5e)$$

where $|\phi_{e0}\rangle$ is an entangled qubit transition state obtained in the form

$$|\phi_{e0}\rangle = c_{e0}|\psi_{e0}\rangle + s_{e0}|\psi_{g1}\rangle ; \quad R_{e0} = g\sqrt{1+\xi^2} ; \quad c_{e0} = \frac{\delta}{2R_{e0}} ; \quad s_{e0} = \frac{g}{R_{e0}} ; \quad \xi = \frac{\delta}{2g} \quad (5f)$$

We identify R_{e0} as the Rabi frequency of the JC qubit oscillations. Repeated application of \hat{A} on $|\psi_{e0}\rangle$ even and odd number times using equation (5e) gives useful general qubit state transition algebraic operations

$$\hat{A}^{2k} |\psi_{e0}\rangle = R_{e0}^{2k} |\psi_{e0}\rangle \quad ; \quad \hat{A}^{2k+1} |\psi_{e0}\rangle = R_{e0}^{2k+1} |\phi_{e0}\rangle \quad ; \quad k = 0, 1, 2, 3, \dots \quad (5g)$$

The general time evolving state $|\Psi_{e0}(t)\rangle$ describing QRM dynamics generated by H_{JC} from the initial state $|\psi_{e0}\rangle$ is obtained in the form

$$|\Psi_{e0}(t)\rangle = U_{JC}(t)|\psi_{e0}\rangle \quad ; \quad U_{JC}(t) = e^{-\frac{it}{\hbar}H_{JC}} \quad (6a)$$

where $U_{JC}(t)$ is the JC time evolution operator which on substituting H_{JC} from equation (5d) and noting the commutation relation $[\hat{N}, \hat{A}] = 0$ takes the factorized form

$$U_{JC}(t) = e^{-it\hat{A}}e^{-i\omega t\hat{N}} \quad (6b)$$

Substituting this into equation (6a) and applying $\hat{N} = \hat{a}^\dagger\hat{a} + s_+s_-$ on $|\psi_{e0}\rangle$ gives

$$\hat{N}|\psi_{e0}\rangle = |\psi_{e0}\rangle \quad \Rightarrow \quad |\Psi_{e0}(t)\rangle = e^{-i\omega t}e^{-it\hat{A}}|\psi_{e0}\rangle \quad (6c)$$

Expanding $e^{-it\hat{A}}$ and reorganizing in even and odd power terms

$$e^{-it\hat{A}} = \sum_{k=0}^{\infty} \frac{(-1)^k t^{2k}}{(2k)!} \hat{A}^{2k} - i \sum_{k=0}^{\infty} \frac{(-1)^k t^{2k+1}}{(2k+1)!} \hat{A}^{2k+1} \quad (6d)$$

and substituting into equation (6c), applying the general qubit state algebraic operations from equation (5g), then introducing standard trigonometric expansions, we obtain the general time evolving state in the final form

$$|\Psi_{e0}(t)\rangle = e^{-i\omega t}(\cos(R_{e0}t)|\psi_{e0}\rangle - i \sin(R_{e0}t)|\phi_{e0}\rangle) \quad (6e)$$

which describes Rabi oscillations at frequency R_{e0} between the initial separable state $|\psi_{e0}\rangle$ and an entangled transition state $|\phi_{e0}\rangle$. Substituting $|\phi_{e0}\rangle$ from equation (5f) into equation (6e), reorganizing and introducing the definitions of $|\psi_{e0}\rangle$, $|\psi_{g1}\rangle$ from equation (5a) reveals that in general, the time evolving state $|\Psi_{e0}(t)\rangle$ is a normalized entangled state obtained in the form

$$|\Psi_{e0}(t)\rangle = e^{-i\omega t}(\cos(R_{e0}t) - ic_{e0}\sin(R_{e0}t)|e0\rangle - is_{e0}\sin(R_{e0}t)|g1\rangle) ; \quad \langle\Psi_{e0}(t)|\Psi_{e0}(t)\rangle = 1 \quad (6f)$$

135 Hence, as we set out to demonstrate, the effective JC Hamiltonian H_{JC} generates dynamical evolution of the
 136 initial atom-field state $|e0\rangle$ into a time evolving entangled state $|\Psi_{e0}(t)\rangle$ in RF. We can now compare QRM
 137 dynamics described by $|\Psi_{e0}(t)\rangle$ in RF to the corresponding dynamical features observed in the JC ($\frac{g}{\omega} = 0.04$)
 138 regime in the QRM simulation experiment in [9]. In this respect, we determine the atomic excitation number,
 139 field mode mean photon number, the JC and AJC excitation numbers in the state $|\Psi_{e0}(t)\rangle$.

Applying the JC excitation number operator \hat{N} on $|\Psi_{e0}(t)\rangle$ gives an eigenvalue equation

$$\hat{N}|\Psi_{e0}(t)\rangle = |\Psi_{e0}(t)\rangle \quad \Rightarrow \quad \overline{N}(t) = 1 \quad (6g)$$

140 from which it follows that the JC excitation number $\overline{N}(t)$ is conserved in the QRM dynamics generated
 141 by the effective JC Hamiltonian H_{JC} in RF as expected from the corresponding commutation relation
 142 $[\hat{N}, H_{JC}] = 0$ in equation (4a). The experiment in [9] confirmed conservation of the JC excitation number
 143 (the only total excitation number known at the time of the experiment) in the corresponding JC regime
 144 characterized by $\frac{g}{\omega} = 0.04$ in [9].

We determine the atomic population inversion $\overline{s}_z(t)$ and excitation number $\overline{s_+s_-}(t)$, the field mode mean photon number $\overline{n}(t)$ and the AJC excitation number $\overline{\overline{N}}(t)$ in the QRM time evolving state $|\Psi_{e0}(t)\rangle$ in RF in the form (recall $s_+s_- = \frac{1}{2} + s_z$; $s_-s_+ = \frac{1}{2} - s_z$)

$$\overline{s}_z(t) = \frac{1}{2}(1 - 2s_{e0}^2 \sin^2(R_{e0}t)) ; \quad \overline{s_+s_-}(t) = \frac{1}{2} + \overline{s}_z(t) ; \quad \overline{n}(t) = s_{e0}^2 \sin^2(R_{e0}t) ; \quad \overline{\overline{N}}(t) = 2(1 - \overline{s}_z(t)) \quad (6h)$$

145 It follows immediately from equation (6h) that the AJC excitation number $\overline{\overline{N}}(t)$ is non-conserved and evolves
 146 in time in the QRM dynamics generated by the effective JC Hamiltonian H_{JC} in RF as expected from the
 147 corresponding commutation relation $[\hat{\overline{N}}, H_{JC}] \neq 0$ in equation (4a). This dynamical evolution was not
 148 investigated in [9], since the authors were not yet aware of the existence of the AJC excitation number
 149 operator as a QRM order parameter at the time of the experiment in [9].

150 The form of dynamical evolution of the atomic excitation number $X = \overline{s_+ s_-}(t)$ and the field mode
 151 mean photon number $F = \overline{n}(t)$, characterized by pure Rabi oscillations in Fig.1 , Fig.2, respectively, agrees
 152 precisely with the corresponding dynamical evolution observed in the JC ($\frac{g}{\omega} = 0.04$) regime in the experiment
 153 in [9]. Fig.3 reveals the conservation of the JC excitation number $\overline{N}(t)$ in RF, agreeing with the behavior
 154 observed in the JC regime in [9]. The dynamical evolution of the AJC excitation number $\overline{\overline{N}}(t)$ in Fig.4 was
 155 not investigated in [9] as we have already explained.

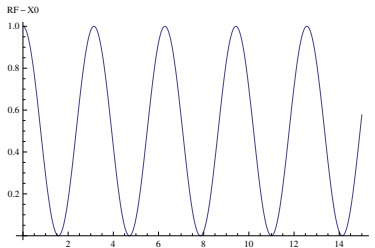


Figure 1: JC-atomic excitation number in RF $\overline{s_+ s_-}(\tau)$, $\tau = gt$: $\xi = 0$; $\varepsilon = \dots$

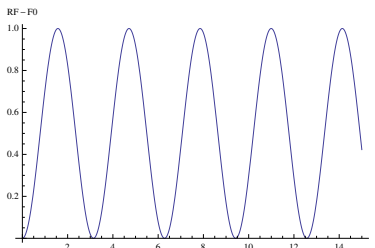


Figure 2: JC-field mode mean photon number in RF $\overline{n}(\tau)$, $\tau = gt$: $\xi = 0$; $\varepsilon = \dots$

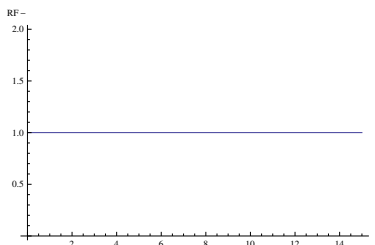


Figure 3: JC-excitation number in RF $\overline{N}(\tau)$, $\tau = gt$: $\xi = 0$; $\varepsilon = \dots$

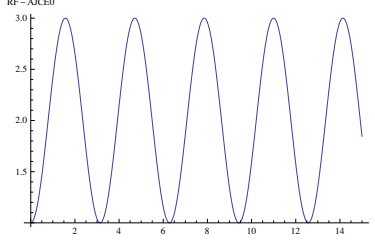


Figure 4: AJC-excitation number in RF $\overline{N}(\tau)$, $\tau = gt$: $\xi = 0$; $\varepsilon = \dots$

156 There are two points to note at this stage: (i) in presenting the dynamical evolution in Fig.1-Fig.4, we have
 157 set the dimensionless coupling parameter $\xi = \frac{\delta}{2g} = 0$ coinciding with $\omega_0 = \omega$ in [9], but the parameter $\varepsilon^{-1} = \frac{g}{\omega}$
 158 used to characterize the coupling regimes in [9] does not affect the dynamical evolution described by $|\Psi_{e0}(t)\rangle$
 159 in RF, noting $\delta = 0$, $\xi = 0$ gives $R_{e0} = g$, $c_{e0} = 0$, $s_{e0} = 1$, $|\Psi_{e0}(t)\rangle = e^{-i\omega t}(\cos(R_{e0}t)|e0\rangle - i\sin(R_{e0}t)|g1\rangle)$
 160 according to equations (5f), (6f) (ii) taking note of the dynamical features of the USC-DSC regimes regarding
 161 the vacuum state [1, 4, 5, 11, 12], the atom-field initial state in [9] is defined with the field mode in a
 162 displaced vacuum state with displacement parameter $\pm \frac{g}{\omega}$, while the atom may be in an eigenstate of the spin
 163 operator $\sigma_x = s_- + s_+$ so that the general dynamical evolution of the atom-field initial state takes the form of
 164 a Schroedinger cat state, which depends on the coupling regime parameter $\frac{g}{\omega}$. Varying $\frac{g}{\omega}$ from the JC to the
 165 USC-DSC regimes then determines the dynamical features of QRM as observed in the three coupling regimes
 166 in [9]. To obtain corresponding dynamical features in the description developed in the present article, we
 167 provide a consistent generalization of the atom-field initial state $|e0\rangle$ to an $n \geq 0$ entangled eigenstate of the
 168 effective AJC Hamiltonian \overline{H}_{AJC} here below.

169 3.1.2 Dynamics from a general initial AJC eigenstate

Noting that the initial state $|\psi_{e0}\rangle$ used above in developing QRM dynamics in RF is an eigenstate of the
 AJC Hamiltonian \overline{H}_{AJC} according to equation (5b), we now provide a consistent generalization to an $n \geq 0$
 initial AJC eigenstate. Since the atom starts in the excited state $|e\rangle$, the basic $n \geq 0$ atom-field state is $|en\rangle$.
 Considering that the state algebraic operation for determining a general eigenstate of the AJC Hamiltonian
 couples the state $|en\rangle$ to the state $|gn-1\rangle$, we introduce appropriate notation $|\psi_{en}\rangle$, $|\psi_{gn-1}\rangle$ for the two
 states in the form

$$|\psi_{en}\rangle = |en\rangle; \quad |\psi_{gn-1}\rangle = |gn-1\rangle \quad (7a)$$

Introducing an AJC qubit state transition operator \hat{A} related to the AJC excitation number operator \hat{N}
 defined by

$$\hat{A} = \bar{\delta}s_z + g(\hat{a}s_- + \hat{a}^\dagger s_+); \quad \hat{A}^2 = \frac{1}{4}\bar{\delta}^2 + g^2(\hat{N} - 1) \quad (7b)$$

we express the effective AJC Hamiltonian \overline{H}_{AJC} in equation (3e) in the form

$$\overline{H}_{AJC} = \hbar\omega(\hat{N} - 1) + \hbar\hat{A} \quad (7c)$$

Applying \hat{A} from equation (7b) on the state $|\psi_{en}\rangle$ in equation (7a), reorganizing, then applying \hat{A} on the
 resulting transition state $|\bar{\phi}_{en}\rangle$, we determine AJC qubit states $|\psi_{en}\rangle$, $|\bar{\phi}_{en}\rangle$ satisfying qubit state algebraic
 operations

$$\hat{A}|\psi_{en}\rangle = \overline{R}_{en}|\bar{\phi}_{en}\rangle; \quad \hat{A}|\bar{\phi}_{en}\rangle = \overline{R}_{en}|\psi_{en}\rangle \quad (7d)$$

where

$$|\bar{\phi}_{en}\rangle = \bar{c}_{en}|\psi_{en}\rangle + \bar{s}_{en}|\psi_{gn-1}\rangle; \quad \overline{R}_{en} = g\sqrt{n + (\xi + \varepsilon)^2}; \quad \bar{c}_{en} = \frac{\bar{\delta}}{2\overline{R}_{en}}; \quad \bar{s}_{en} = \frac{g\sqrt{n}}{\overline{R}_{en}}; \quad \varepsilon = \frac{\omega}{g} \quad (7e)$$

170 where we have rewritten $\bar{\delta} = \delta + 2\omega$, $\bar{\delta}/2g = \delta/2g + \omega/g$ and the parameter $\xi = \delta/2g$ is defined in equation
 171 (5f). We identify \overline{R}_{en} as the Rabi frequency of oscillations between the AJC qubit states $|\psi_{en}\rangle$, $|\bar{\phi}_{en}\rangle$, well
 172 developed in [7, 8] and in subsection 3.2 below.

Noting that the qubit states $|\psi_{en}\rangle$, $|\bar{\phi}_{en}\rangle$ are non-orthogonal satisfying

$$\langle\psi_{en}|\psi_{en}\rangle = 1, \quad \langle\psi_{en}|\bar{\phi}_{en}\rangle = \bar{c}_{en}, \quad \langle\bar{\phi}_{en}|\psi_{en}\rangle = \bar{c}_{en}, \quad \langle\bar{\phi}_{en}|\bar{\phi}_{en}\rangle = 1 \quad (7f)$$

we introduce normalized AJC eigenstates $|\bar{\Psi}_{en}^+\rangle$, $|\bar{\Psi}_{en}^-\rangle$ obtained as simple linear combinations of the qubit states in the form

$$|\bar{\Psi}_{en}^+\rangle = \frac{1}{\sqrt{2(1+\bar{c}_{en})}} (|\psi_{en}\rangle + |\bar{\phi}_{en}\rangle); \quad |\bar{\Psi}_{en}^-\rangle = \frac{1}{\sqrt{2(1-\bar{c}_{en})}} (|\psi_{en}\rangle - |\bar{\phi}_{en}\rangle) \quad (7g)$$

satisfying eigenvalue equations

$$\begin{aligned} \hat{A} |\bar{\Psi}_{en}^\pm\rangle &= \pm \bar{R}_{en} |\bar{\Psi}_{en}^\pm\rangle; & \hat{N} |\bar{\Psi}_{en}^\pm\rangle &= (n+1) |\bar{\Psi}_{en}^\pm\rangle \\ \bar{H}_{AJC} |\bar{\Psi}_{en}^\pm\rangle &= \bar{E}_{en}^\pm |\bar{\Psi}_{en}^\pm\rangle; & \bar{E}_{en}^\pm &= \hbar\omega n \pm \hbar\bar{R}_{en} \end{aligned} \quad (7h)$$

If we now set $n=0$ in equations (7e), (7g), (7h), the general $n \geq 0$ eigenstates $|\bar{\Psi}_{en}^\pm\rangle$ reduce to the forms (recalling $\bar{\delta} = \omega_0 + \omega$)

$$\begin{aligned} n=0 : \quad |\bar{\Psi}_{en}^+\rangle &\rightarrow |\bar{\Psi}_{e0}^+\rangle = |\psi_{e0}\rangle; & \bar{E}_{e0}^+ &= \frac{1}{2}\hbar(\omega_0 + \omega) \\ |\bar{\Psi}_{en}^-\rangle &\rightarrow |\bar{\Psi}_{e0}^-\rangle = 0; & \bar{E}_{e0}^- &= -\frac{1}{2}\hbar(\omega_0 + \omega) \end{aligned} \quad (7i)$$

173 which show that $|\bar{\Psi}_{en}^+\rangle$ is the general $n \geq 0$ AJC eigenstate which reduces to the $n=0$ initial state $|\psi_{e0}\rangle$
 174 with the correct AJC energy eigenvalue $\bar{E}_{e0}^+ = \frac{1}{2}\hbar(\omega_0 + \omega)$ agreeing precisely with equation (5b). Notice that
 175 for $n=0$, the eigenstate $|\bar{\Psi}_{en}^-\rangle$ reduces to $|\bar{\Psi}_{e0}^-\rangle = 0$ specified by energy eigenvalue $\bar{E}_{e0}^- = -\frac{1}{2}\hbar(\omega_0 + \omega)$
 176 which may represent a closed state in the lower AJC spectrum with the atom in the normal ground state of
 177 energy $-\frac{1}{2}\hbar\omega_0$ and the field mode in the *antinormal* vacuum state of negative energy $-\frac{1}{2}\hbar\omega$.

From equation (7i), we identify $|\bar{\Psi}_{en}^+\rangle$ in equation (7g) as the consistent $n \geq 0$ generalization of the AJC eigenstate defining the general initial state for general QRM dynamics generated by the effective JC Hamiltonian H_{JC} in RF which we now present below. In this respect, we substitute the definition of $|\bar{\phi}_{en}\rangle$ from equation (7e) into equation (7g) and reorganize to express $|\bar{\Psi}_{en}^+\rangle$ in the form

$$|\bar{\Psi}_{en}^+\rangle = \frac{1}{\sqrt{2(1+\bar{c}_{en})}} ((1+\bar{c}_{en})|\psi_{en}\rangle + \bar{s}_{en}|\psi_{gn-1}\rangle) \quad (7j)$$

178 Substituting the definitions of $|\psi_{en}\rangle$, $|\psi_{gn-1}\rangle$ from equation (7a) reveals that $|\bar{\Psi}_{en}^+\rangle$ is an entangled state.
 179 Note that choosing an AJC eigenstate as the initial state inactivates the AJC interaction in the QRM
 180 dynamics in RF, noting that according to the eigenvalue equation (7h), \bar{H}_{AJC} generates only plane wave
 181 evolution $e^{-\frac{i}{\hbar}E_{en}^+t}|\bar{\Psi}_{en}^+\rangle$.

The general time evolving state $|\Psi_{RF}(t)\rangle$ of general QRM dynamics in RF is generated from the general initial $n \geq 0$ AJC eigenstate $|\bar{\Psi}_{en}^+\rangle$ through the effective JC Hamiltonian H_{JC} according to

$$|\Psi_{RF}(t)\rangle = U_{JC}(t) |\bar{\Psi}_{en}^+\rangle \quad (8a)$$

where the time evolution operator $U_{JC}(t)$ is defined in equations (6a)-(6b). Substituting $|\bar{\Psi}_{en}^+\rangle$ from equation (7j) into equation (8a) gives the form

$$\begin{aligned} |\Psi_{RF}(t)\rangle &= \frac{1}{\sqrt{2(1+\bar{c}_{en})}} ((1+\bar{c}_{en})|\Psi_{en}(t)\rangle + \bar{s}_{en}|\Psi_{gn-1}(t)\rangle) \\ |\Psi_{en}(t)\rangle &= U_{JC}(t)|\psi_{en}\rangle; & |\Psi_{gn-1}(t)\rangle &= U_{JC}(t)|\psi_{gn-1}\rangle \end{aligned} \quad (8b)$$

Applying the JC qubit state transition operator \hat{A} from equation (5c) on $|\psi_{en}\rangle$, $|\psi_{gn-1}\rangle$ generates the respective qubit states $(|\psi_{en}\rangle, |\phi_{en}\rangle)$, $(|\psi_{gn-1}\rangle, |\phi_{gn-1}\rangle)$ satisfying state transition algebraic operations

$$\begin{aligned} \hat{A} |\psi_{en}\rangle &= R_{en+1}|\phi_{en}\rangle; & \hat{A} |\phi_{en}\rangle &= R_{en+1}|\psi_{en}\rangle; & |\phi_{en}\rangle &= c_{en+1}|\psi_{en}\rangle + s_{en+1}|\psi_{gn+1}\rangle \\ |\psi_{gn+1}\rangle &= |gn+1\rangle; & R_{en+1} &= g\sqrt{(n+1)+\xi^2}; & c_{en+1} &= \frac{\delta}{2R_{en+1}}; & s_{en+1} &= \frac{g\sqrt{n+1}}{R_{en+1}} \end{aligned} \quad (8c)$$

$$\begin{aligned} \hat{A} |\psi_{gn-1}\rangle &= R_{gn-1} |\phi_{gn-1}\rangle ; & \hat{A} |\phi_{gn-1}\rangle &= R_{gn-1} |\psi_{gn-1}\rangle ; & |\phi_{gn-1}\rangle &= -c_{gn-1} |\psi_{gn-1}\rangle + s_{gn-1} |\psi_{en-2}\rangle \\ |\psi_{en-2}\rangle &= |en-2\rangle ; & R_{gn-1} &= g\sqrt{(n-1) + \xi^2} ; & c_{gn-1} &= \frac{\delta}{2R_{gn-1}} ; & s_{gn-1} &= \frac{g\sqrt{n-1}}{R_{gn-1}} \end{aligned} \quad (8d)$$

182 where R_{en+1} , R_{gn-1} are the respective Rabi frequencies of qubit oscillations.

Substituting $U_{JC}(t)$ from equation (6b) into equation (8b), noting

$$\hat{N} |\psi_{en}\rangle = (n+1) |\psi_{en}\rangle ; \quad \hat{N} |\psi_{gn-1}\rangle = (n-1) |\psi_{gn-1}\rangle \quad (8e)$$

and using equation (6d) with repeated application of \hat{A} on $|\psi_{en}\rangle$, $|\psi_{gn-1}\rangle$ even and odd number of times, giving general qubit state algebraic relations similar to the relations in equation (5g), then introducing trigonometric functions according to the expansions as appropriate, we obtain

$$\begin{aligned} |\Psi_{en}(t)\rangle &= e^{-i\omega(n+1)t} (\cos(R_{en+1}t) |\psi_{en}\rangle - i \sin(R_{en+1}t) |\phi_{en}\rangle) \\ |\Psi_{gn-1}(t)\rangle &= e^{-i\omega(n-1)t} (\cos(R_{gn-1}t) |\psi_{gn-1}\rangle - i \sin(R_{gn-1}t) |\phi_{gn-1}\rangle) \end{aligned} \quad (8f)$$

183 Substituting these into equation (8b) provides the explicit form of the general time evolving QRM state
184 $|\Psi_{RF}(t)\rangle$ in RF generated by the effective JC Hamiltonian H_{JC} from the general $n \geq 0$ entangled AJC eigen-
185 state $|\bar{\Psi}_{en}^+\rangle$ according to equation (8a). Introducing the definitions of the states ($|\psi_{en}\rangle$, $|\psi_{gn+1}\rangle$, $|\phi_{en}\rangle$)
186 and ($|\psi_{gn-1}\rangle$, $|\psi_{en-2}\rangle$, $|\phi_{gn-1}\rangle$) from equations (7a), (8c), (8d) reveals that $|\Psi_{RF}(t)\rangle$ is a general time
187 evolving entangled state.

We easily obtain orthonormalization relations

$$\begin{aligned} \langle \Psi_{en}(t) | \Psi_{en}(t) \rangle &= 1 ; & \langle \Psi_{en}(t) | \Psi_{gn-1}(t) \rangle &= 0 ; & \langle \Psi_{gn-1}(t) | \Psi_{en}(t) \rangle &= 0 ; & \langle \Psi_{gn-1}(t) | \Psi_{gn-1}(t) \rangle &= 1 \\ \langle \Psi_{RF}(t) | \Psi_{RF}(t) \rangle &= 1 \end{aligned} \quad (8g)$$

We obtain the JC excitation number $\bar{N}(t)$ in the general time evolving QRM state $|\Psi_{RF}(t)\rangle$ in the form

$$\bar{N}(t) = n + 1 - \frac{\bar{s}_{en}^2}{1 + \bar{c}_{en}} \quad (8h)$$

which once again confirms that the JC excitation number is conserved in RF as expected according to the commutation relation $[\hat{N}, H_{JC}] = 0$ in equation (4a). The atomic population inversion and excitation $\bar{s}_z(t)$, $\bar{s}_+ \bar{s}_-(t)$, the field mode mean photon number $\bar{n}(t)$ and the AJC excitation number $\bar{N}(t)$ in the general QRM state $|\Psi_{RF}(t)\rangle$ in RF are obtained in the form

$$\begin{aligned} \bar{s}_z(t) &= \frac{1}{4(1 + \bar{c}_{en})} \{ (1 + \bar{c}_{en})^2 (1 - 2s_{en+1}^2 \sin^2(R_{en+1}t)) - \bar{s}_{en}^2 (1 - 2s_{gn-1}^2 \sin^2(R_{gn-1}t)) \} \\ \bar{s}_+ \bar{s}_-(t) &= \frac{1}{2} + \bar{s}_z(t) ; & \bar{n}(t) &= n + \frac{1}{2} - \frac{\bar{s}_{en}^2}{1 + \bar{c}_{en}} - \bar{s}_z(t) ; & \bar{N}(t) &= n - \frac{\bar{s}_{en}^2}{1 + \bar{c}_{en}} + 2(1 - \bar{s}_z(t)) \end{aligned} \quad (8i)$$

188 We observe that setting $n = 0$ reduces $|\Psi_{RF}(t)\rangle$ in equation (8b) to $|\Psi_{e0}(t)\rangle$ in equation (6e), (6f) and the
189 results in equation ((8i) reduce to the corresponding results in equation (6h), showing that QRM dynamical
190 evolution from the general $n \geq 0$ entangled AJC eigenstate $|\bar{\Psi}_{en}^+\rangle$ in equation (7j) is a consistent generaliza-
191 tion of the dynamical evolution from the $n = 0$ AJC eigenstate $|\psi_{e0}\rangle$ in equation (5a). Plots of the excitation
192 numbers in equation (8i) for initial field mode photon number $n = 0$ reproduce the corresponding plots in
193 Fig.1-Fig.4.

194 For initial photon numbers $n \geq 1$, the time evolution of the excitation numbers in equation (8i) is
195 characterized by quantum collapses and revivals largely determined by the field mode initial photon number
196 n , which we display for the arbitrarily chosen case $n = 40$ in Fig.5-Fig.7 for the atomic excitation number
197 $X = \bar{s}_+ \bar{s}_-(t)$, field mode mean photon number $F = \bar{n}(t)$ and the AJC excitation number $\bar{N}(t)$, respectively.
198 In contrast to the collapse and revival phenomena in the USC-DSC regime due to specification of the atom-
199 field initial state with field mode in initial displaced vacuum state in [9], the collapse and revival phenomenon
200 revealed here in Fig.5-Fig.7 is due to the superposition of time evolving entangled states $|\Psi_{en}(t)\rangle$, $|\Psi_{gn-1}(t)\rangle$
201 with competing Rabi frequencies R_{en+1} , R_{gn-1} which constitute the general QRM state $|\Psi_{RF}(t)\rangle$ in RF
202 according to equations (8b), (8f). We observe that the collapses and revivals in Fig.5-Fig.7 agree particularly
203 well with the field mode mean photon number collapses and revivals obtained in [1].

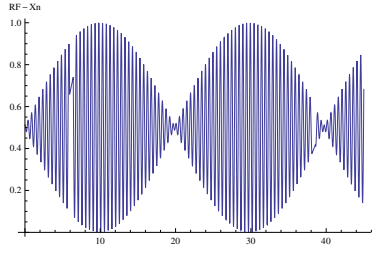


Figure 5: JC-atomic excitation number in RF $\overline{s_+s_-}(\tau)$, $\tau = gt$: $\xi = 0$; $\varepsilon = \dots$; $n = 40$

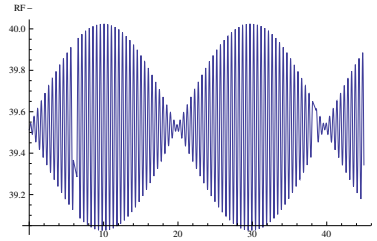


Figure 6: JC-field mode mean photon number in RF $\overline{n}(\tau)$, $\tau = gt$: $\xi = 0$; $\varepsilon = \dots$; $n = 40$

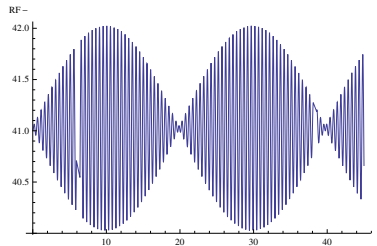


Figure 7: AJC-excitation number in RF $\overline{N}(\tau)$, $\tau = gt$: $\xi = 0$; $\varepsilon = \dots$; $n = 40$

204 We note that the collapse-revival phenomenon revealed here in Fig.5-Fig.7 is a familiar dynamical feature
 205 of JC interaction mechanism for atom-field initial states formed from superpositions of atom or field mode
 206 states with specified initial photon distributions, which may not be related in any way to the interaction
 207 mechanisms in the USC-DSC regimes of QRM as generally defined in [1 , 2 , 4 , 9-15]. QRM dynamics in
 208 the USC-DSC regime has generally been associated with the AJC component, but without specifying how
 209 the AJC interaction generates dynamical evolution from an initial state, which we now present in the next
 210 subsection.

211 3.2 QRM dynamics in CRF

212 We have established in subsection 2.3 that QRM dynamics in CRF is generated by the effective AJC Hamil-
 213 tonian \bar{H}_{JC} in CRWA according to equations (3e)-(3f). We note that various theoretical and experimental
 214 studies of QRM beyond the RWA have characterized CRF as the USC-DSC regime [1 , 2 , 4 , 9-15]. With
 215 this USC-DSC characterization in mind, we follow the experiments [9-12] in identifying and using the state
 216 $|g0\rangle$ with the field mode in the vacuum state $|0\rangle$ and the atom in the ground state $|g\rangle$ as the appropriate
 217 initial state for QRM dynamics in CRF. Here, we establish that the initial state $|g0\rangle$ in CRF is an eigenstate
 218 of the effective JC Hamiltonian H_{JC} and provide a consistent generalization to the corresponding $n \geq 0$
 219 initial JC eigenstate which reduces to $|g0\rangle$ for $n = 0$.

220 3.2.1 Dynamics from initial state $|g0\rangle$

We introduce appropriate notation $|\psi_{g0}\rangle$ for the initial state and $|\psi_{e1}\rangle$ for the associated transition state
 defined in standard notation as

$$|\psi_{g0}\rangle = |g0\rangle \quad ; \quad |\psi_{e1}\rangle = |e1\rangle \quad (9a)$$

Determining the dynamical evolution of the QRM ground state $|g0\rangle$ has been problematic, noting that the
 effective JC Hamiltonian H_{JC} cannot generate dynamical evolution of $|g0\rangle$ in CRF, since this initial state
 is an eigenstate of H_{JC} . Indeed, using H_{JC} from equation (3b) and applying standard atom and field mode
 state algebraic operations, we easily establish that the QRM ground state $|\psi_{g0}\rangle$ is an eigenstate of the effective
 JC Hamiltonian satisfying an eigenvalue equation (recall $\delta = \omega_0 - \omega$)

$$H_{JC}|\psi_{g0}\rangle = -\frac{1}{2}\hbar(\omega_0 - \omega)|\psi_{g0}\rangle \quad (9b)$$

221 where we identify the energy eigenvalue $-\frac{1}{2}\hbar(\omega_0 - \omega)$ as the atomic ground state energy $-\frac{1}{2}\hbar\omega_0$ and the
 222 field mode vacuum state energy $\frac{1}{2}\hbar\omega$ as expected. Equation (9b) means that the effective JC Hamiltonian
 223 H_{JC} generates only plane wave evolution $e^{\frac{i\hbar}{2}(\omega_0 - \omega)t}|\psi_{g0}\rangle$ of the initial state $|\psi_{g0}\rangle$ which does not describe
 224 the general QRM dynamics in CRF. However, the effective AJC Hamiltonian \bar{H}_{AJC} generates dynamical
 225 evolution of the initial state $|\psi_{g0}\rangle$ into a time evolving entangled state which describes the general QRM
 226 dynamics in CRF as we now demonstrate.

We recall the AJC qubit state transition operator \hat{A} and effective Hamiltonian \bar{H}_{AJC} as defined in
 equations (7b)-(7c), which we now rewrite here for ease of reference as

$$\hat{A} = \bar{\delta}s_z + g(\hat{a}s_- + \hat{a}^\dagger s_+) ; \quad \hat{A}^2 = \frac{1}{4}\bar{\delta}^2 + g^2(\hat{N} - 1) ; \quad \bar{H}_{AJC} = \hbar\omega(\hat{N} - 1) + \hbar\hat{A} \quad (9c)$$

227 Conservation of the AJC excitation number in the dynamics generated by \bar{H}_{AJC} in CRF is easily proved by
 228 using the relations in equation (9c) to show that \hat{N} commutes with \bar{H}_{AJC} , thus confirming equations (2f) ,
 229 (4a) and here again simplifying the earlier proof in [6].

Applying \hat{A} from equation (9c) on the initial state $|\psi_{g0}\rangle$ defined in equation (9a), using standard atom-
 field state algebraic operations and reorganizing as appropriate, we obtain AJC qubit states $|\psi_{g0}\rangle$, $|\bar{\phi}_{g0}\rangle$
 satisfying qubit state transition algebraic operations in the form

$$\hat{A}|\psi_{g0}\rangle = \bar{R}_{g0}|\bar{\phi}_{g0}\rangle ; \quad \hat{A}|\bar{\phi}_{g0}\rangle = \bar{R}_{g0}|\psi_{g0}\rangle \quad (9d)$$

where $|\bar{\phi}_{g0}\rangle$ is an entangled qubit transition state obtained in the form

$$|\bar{\phi}_{g0}\rangle = -\bar{c}_{g0}|\psi_{g0}\rangle + \bar{s}_{g0}|\psi_{e1}\rangle ; \quad \bar{R}_{g0} = g\sqrt{1 + (\xi + \varepsilon)^2} ; \quad \bar{c}_{g0} = \frac{\bar{\delta}}{2\bar{R}_{g0}} ; \quad \bar{s}_{g0} = \frac{g}{\bar{R}_{g0}} \quad (9e)$$

The general time evolving state $|\bar{\Psi}_{g0}(t)\rangle$ describing QRM dynamics generated by \bar{H}_{AJC} from the initial state $|\psi_{g0}\rangle$ is obtained in the form

$$|\bar{\Psi}_{g0}(t)\rangle = \bar{U}_{AJC}(t)|\psi_{g0}\rangle ; \quad \bar{U}_{AJC}(t) = e^{-\frac{it}{\hbar}\bar{H}_{AJC}} \quad (10a)$$

where $\bar{U}_{AJC}(t)$ is the AJC time evolution operator which on substituting \bar{H}_{AJC} from equation (9c) and noting the commutation relation $[\hat{N}, \hat{A}] = 0$ takes the factorized form

$$\bar{U}_{AJC}(t) = e^{-it\hat{A}}e^{-i\omega t(\hat{N}-1)} \quad (10b)$$

Substituting this into equation (10a) and applying $\hat{N} = \hat{a}\hat{a}^\dagger + s_-s_+$ on $|\psi_{g0}\rangle$ gives

$$(\hat{N} - 1)|\psi_{g0}\rangle = |\psi_{g0}\rangle \quad \Rightarrow \quad |\bar{\Psi}_{g0}(t)\rangle = e^{-i\omega t}e^{-it\hat{A}}|\psi_{g0}\rangle \quad (10c)$$

Expanding $e^{-it\hat{A}}$ in even and odd power terms similar to the corresponding JC time evolution operator expansion in equation (6d) and substituting into equation (10c), we apply \hat{A} on $|\psi_{g0}\rangle$ even and odd number of times using the qubit state transition algebraic operations from equation (9d) giving relations similar to equation (5g) and then introduce trigonometric functions in the expansions as appropriate to obtain the general time evolving state in the final form

$$|\bar{\Psi}_{g0}(t)\rangle = e^{-i\omega t}(\cos(\bar{R}_{g0}t)|\psi_{g0}\rangle - i\sin(\bar{R}_{g0}t)|\bar{\phi}_{g0}\rangle) \quad (10d)$$

which describes Rabi oscillations at frequency \bar{R}_{g0} between the initial separable state $|\psi_{g0}\rangle$ and the entangled transition state $|\bar{\phi}_{g0}\rangle$. Substituting $|\bar{\phi}_{g0}\rangle$ from equation (9e) into equation (10d), reorganizing and introducing the definitions of $|\psi_{g0}\rangle$, $|\psi_{e1}\rangle$ from equation (9a) reveals that in general, the time evolving state $|\bar{\Psi}_{g0}(t)\rangle$ is a normalized entangled state obtained in the form

$$|\bar{\Psi}_{g0}(t)\rangle = e^{-i\omega t}(\cos(\bar{R}_{g0}t) + i\bar{c}_{g0}\sin(\bar{R}_{g0}t)|g0\rangle - i\bar{s}_{g0}\sin(\bar{R}_{g0}t)|e1\rangle); \quad \langle \bar{\Psi}_{g0}(t)|\bar{\Psi}_{g0}(t)\rangle = 1 \quad (10e)$$

230 Hence, as we set out to demonstrate, the effective AJC Hamiltonian \bar{H}_{AJC} generates dynamical evolution of
 231 the initial atom-field state $|g0\rangle$ into a time evolving entangled state $|\bar{\Psi}_{g0}(t)\rangle$ in CRF. We observe that this
 232 form of dynamical evolution of the QRM ground state $|g0\rangle$ into a time evolving entangled state generated
 233 by the effective AJC Hamiltonian has never been determined in the various theoretical models or related
 234 experiments in [1, 2, 4, 9-15] and others, noting that the solution procedure for AJC interaction has
 235 only been developed by the present author in recent work [6-8]. As we pointed out earlier, considering the
 236 dynamical features of QRM in the USC-DSC regime, the authors of studies in [1, 2, 4, 9-15] defined the
 237 initial atom-field ground state $|g0\rangle$ in a more general form with the field mode in initial displaced vacuum
 238 state and the atom in initial eigenstate of the spin operator $\sigma_x = s_- + s_+$, so that the ground state evolves
 239 into a Schroedinger cat state in the USC-DSC regime [9, 12, 14, 15]. Comparison of QRM dynamics
 240 described by $|\bar{\Psi}_{g0}(t)\rangle$ in CRF with the dynamical features observed in the USC-DSC regime in the QRM
 241 simulation experiments in [9-12] may therefore be inappropriate, since the definition of CRF as a dynamical
 242 frame of QRM as we have developed it in this article is independent of the coupling parameter $\frac{g}{\omega}$ used to
 243 characterize the QRM coupling regimes in [1, 2, 4, 9-15], meaning that CRF may not be equivalent to the
 244 USC-DSC regime. With this in mind, we determine the atomic excitation number, field mode mean photon
 245 number, the JC and AJC excitation numbers to study QRM dynamical features in the state $|\Psi_{g0}(t)\rangle$ in CRF.

Applying the AJC excitation number operator \hat{N} on $|\bar{\Psi}_{g0}(t)\rangle$ gives an eigenvalue equation

$$\hat{N}|\bar{\Psi}_{g0}(t)\rangle = 2|\bar{\Psi}_{g0}(t)\rangle \quad \Rightarrow \quad \bar{\bar{N}}(t) = 2 \quad (10f)$$

246 from which it follows that the AJC excitation number $\bar{\bar{N}}(t)$ is conserved in the QRM dynamics generated
 247 by the effective AJC Hamiltonian \bar{H}_{AJC} in CRF as expected from the corresponding commutation relation
 248 $[\hat{N}, \bar{H}_{AJC}] = 0$ in equation (4a). This property has never been investigated experimentally, since, as we
 249 have explained earlier, the AJC excitation number operator has largely been unknown to both theoreticians
 250 and experimentalists, a fact which has necessitated the work presented in this article.

Noting that AJC operators are defined in antinormal order form, we determine the atomic population inversion $\bar{s}_z(t)$ and antinormal order excitation number $\bar{s}_- \bar{s}_+(t)$, the field mode antinormal order photon

number $\overline{aa^*}(t) = \overline{n}(t) + 1$ and the JC excitation number $\overline{N}(t)$ (normal order) in the QRM time evolving state $|\overline{\Psi}_{g0}(t)\rangle$ in CRF in the form (recall $s_+s_- = \frac{1}{2} + s_z$; $s_-s_+ = \frac{1}{2} - s_z$; $\hat{a}\hat{a}^\dagger = \hat{a}^\dagger\hat{a} + 1$)

$$\begin{aligned} \overline{s}_z(t) &= -\frac{1}{2}(1 - 2\overline{s}_{g0}^2 \sin^2(\overline{R}_{g0}t)) ; & \overline{s_-s_+}(t) &= \frac{1}{2} - \overline{s}_z(t) ; & \overline{n}(t) &= \overline{s}_{g0}^2 \sin^2(\overline{R}_{g0}t) ; & \overline{aa^*}(t) &= 1 + \overline{n}(t) \\ \overline{N}(t) &= \overline{n}(t) + \frac{1}{2} + \overline{s}_z(t) \end{aligned} \quad (10g)$$

251 It follows from equation (10g) that the JC excitation number $\overline{N}(t)$ is non-conserved and evolves in time
 252 in the QRM dynamics generated by the effective AJC Hamiltonian \overline{H}_{AJC} in CRF as expected from the
 253 corresponding commutation relation $[\hat{N}, \overline{H}_{AJC}] \neq 0$ in equation (4a). Experiments [9] have established
 254 that the JC excitation number $\overline{N}(t)$ is conserved in the JC regime corresponding to RF here, but evolves in
 255 time in the USC-DSC regime, which is associated with, but not necessarily equivalent to CRF. In general,
 256 the experimental observations agree with the results we have obtained in equations (6g) , (8h) in RF and
 257 here in equation (10g) in CRF. Here, we now only mention the familiar and overemphasized fact that the
 258 non-conservation of the AJC excitation number $\overline{N}(t)$ in equations (6h) , (8i) in RF and its conservation
 259 determined here in equation (10f) in CRF has not been investigated in experiments.

260 We have plotted the antinormal atomic excitation number $X = \overline{s_-s_+}(t)$, the field mode mean antinormal
 261 photon number $F = \overline{aa^*}(t)$, the AJC and JC excitation numbers $\overline{N}(t)$, $\overline{N}(t)$ from equation (10g) in Fig.8-
 262 Fig.11, respectively. We notice the striking similarity with the time evolution of corresponding quantities
 263 determined in the JC interaction in RF plotted in Fig.1-Fig.4. The similarity in the form of time evolution is
 264 that the excitation and mean photon numbers are defined in quadratic form in both JC and AJC interactions.
 265 We observe that the non-quadratic atomic state population inversion $\overline{s}_z(t)$ and the coherence functions \overline{s}_x ,
 266 $\overline{s}_y(t)$ obtained in JC and AJC interactions in RF , CRF evolve in time in reverse order, which we have not
 267 plotted.

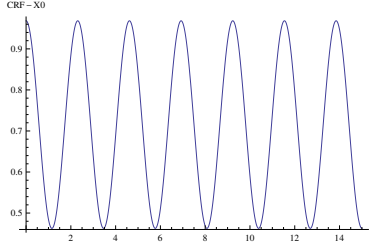


Figure 8: AJC-atomic antinormal excitation number in CRF $\overline{s_-s_+}(\tau)$, $\tau = gt$: $\xi = \frac{1}{1.31}$; $\varepsilon = 0.16$; $n = 0$

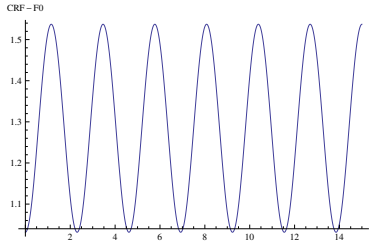


Figure 9: AJC-field mode mean antinormal photon number in CRF $\overline{aa^*}(\tau)$, $\tau = gt$: $\xi = \frac{1}{1.31}$; $\varepsilon = 0.16$; $n = 0$

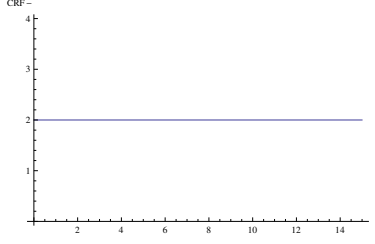


Figure 10: AJC-excitation number in CRF $\overline{N}(\tau)$, $\tau = gt$: $\xi = \frac{1}{1.31}$; $\varepsilon = 0.16$; $n = 0$

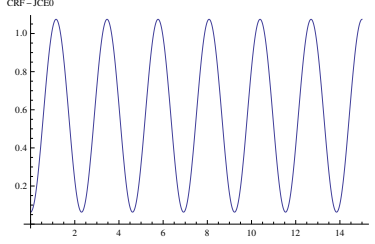


Figure 11: JC-excitation number in CRF $\overline{N}(\tau)$, $\tau = gt$: $\xi = \frac{1}{1.31}$; $\varepsilon = 0.16$; $n = 0$

268 We now generalize the initial atom-field state by determining the $n \geq 0$ JC eigenstate which reduces to
 269 the ground state $|g0\rangle$ at $n = 0$.

270 3.2.2 Dynamics from a general initial JC eigenstate

Noting that the initial state $|\psi_{00}\rangle$ used above in developing QRM dynamics in CRF is an eigenstate of the JC Hamiltonian H_{JC} according to equation (9b), we now provide a consistent generalization to an $n \geq 0$ initial JC eigenstate. Since the atom starts in the ground state $|g\rangle$, the basic $n \geq 0$ atom-field state is $|gn\rangle$. Considering that the state algebraic operation for determining a general eigenstate of the JC Hamiltonian couples the state $|gn\rangle$ to the state $|en - 1\rangle$, we introduce appropriate notation $|\psi_{gn}\rangle$, $|\psi_{en-1}\rangle$ for the two states in the form

$$|\psi_{gn}\rangle = |gn\rangle; \quad |\psi_{en-1}\rangle = |en - 1\rangle \quad (11a)$$

Applying the JC qubit state transition operator \hat{A} from equation (5c) on the state $|\psi_{gn}\rangle$ in equation (11a), reorganizing, then applying \hat{A} on the resulting transition state $|\phi_{gn}\rangle$, we determine JC qubit states $|\psi_{gn}\rangle$, $|\phi_{gn}\rangle$ satisfying qubit state algebraic operations

$$\hat{A} |\psi_{gn}\rangle = R_{gn} |\phi_{gn}\rangle; \quad \hat{A} |\phi_{gn}\rangle = R_{gn} |\psi_{gn}\rangle \quad (11b)$$

where

$$|\phi_{gn}\rangle = -c_{gn} |\psi_{gn}\rangle + s_{gn} |\psi_{en-1}\rangle; \quad R_{gn} = g\sqrt{n + \xi^2}; \quad c_{gn} = \frac{\delta}{2R_{gn}}; \quad s_{gn} = \frac{g\sqrt{n}}{R_{gn}} \quad (11c)$$

Noting that the qubit states $|\psi_{gn}\rangle$, $|\phi_{gn}\rangle$ are non-orthogonal satisfying

$$\langle \psi_{gn} | \psi_{gn} \rangle = 1, \quad \langle \psi_{gn} | \phi_{gn} \rangle = -c_{gn}, \quad \langle \phi_{gn} | \psi_{gn} \rangle = -c_{gn}, \quad \langle \phi_{gn} | \phi_{gn} \rangle = 1 \quad (11d)$$

we introduce normalized JC eigenstates $|\Psi_{gn}^+\rangle$, $|\Psi_{gn}^-\rangle$ obtained as simple linear combinations of the qubit states in the form

$$|\Psi_{gn}^+\rangle = \frac{1}{\sqrt{2(1 - c_{gn})}} (|\psi_{gn}\rangle + |\phi_{gn}\rangle); \quad |\Psi_{gn}^-\rangle = \frac{1}{\sqrt{2(1 + c_{gn})}} (|\psi_{gn}\rangle - |\phi_{gn}\rangle) \quad (11e)$$

satisfying eigenvalue equations

$$\hat{A} |\Psi_{gn}^\pm\rangle = \pm R_{gn} |\Psi_{gn}^\pm\rangle; \quad \hat{N} |\Psi_{gn}^\pm\rangle = n |\Psi_{gn}^\pm\rangle$$

$$H_{JC} |\Psi_{gn}^{\pm}\rangle = E_{gn}^{\pm} |\Psi_{gn}^{\pm}\rangle ; \quad E_{gn}^{\pm} = \hbar\omega n \pm \hbar R_{gn} \quad (11f)$$

If we now set $n = 0$ in equations (11c) , (11e) , (11f), the general $n \geq 0$ eigenstates $|\Psi_{gn}^{\pm}\rangle$ reduce to the forms (recalling $\delta = \omega_0 - \omega$)

$$\begin{aligned} n = 0 : \quad |\Psi_{gn}^+\rangle &\rightarrow |\Psi_{g0}^+\rangle = 0 ; \quad E_{g0}^+ = \frac{1}{2}\hbar(\omega_0 - \omega) \\ |\Psi_{gn}^-\rangle &\rightarrow |\Psi_{g0}^-\rangle = |\psi_{g0}\rangle ; \quad E_{g0}^- = -\frac{1}{2}\hbar(\omega_0 - \omega) \end{aligned} \quad (11g)$$

271 which show that $|\Psi_{gn}^-\rangle$ is the general $n \geq 0$ JC eigenstate which reduces to the $n = 0$ initial state $|\psi_{g0}\rangle$ with
 272 the correct JC energy eigenvalue $E_{g0}^- = -\frac{1}{2}\hbar(\omega_0 - \omega)$ agreeing precisely with equation (9b). Notice that for
 273 $n = 0$, the eigenstate $|\Psi_{gn}^+\rangle$ reduces to $|\Psi_{g0}^+\rangle = 0$ specified by energy eigenvalue $E_{g0}^+ = \frac{1}{2}\hbar(\omega_0 - \omega)$ which
 274 may represent a closed state in the upper JC spectrum with the atom in the normal excited state of energy
 275 $\frac{1}{2}\hbar\omega_0$ and the field mode in the *antinormal* vacuum state of negative energy $-\frac{1}{2}\hbar\omega$.

From equation (11g), we identify $|\Psi_{gn}^-\rangle$ in equation (11e) as the consistent $n \geq 0$ generalization of the JC eigenstate defining the general initial state for general QRM dynamics generated by the effective AJC Hamiltonian \bar{H}_{AJC} in CRF which we now present below. In this respect, we substitute the definition of $|\phi_{gn}\rangle$ from equation (11c) into equation (11e) and reorganize to express $|\Psi_{gn}^-\rangle$ in the form

$$|\Psi_{gn}^-\rangle = \frac{1}{\sqrt{2(1+c_{gn})}} ((1+c_{gn})|\psi_{gn}\rangle - s_{gn}|\psi_{en-1}\rangle) \quad (11h)$$

276 Substituting the definitions of $|\psi_{gn}\rangle$, $|\psi_{en-1}\rangle$ from equation (11a) reveals that $|\Psi_{gn}^-\rangle$ is an entangled state.
 277 Note that choosing a JC eigenstate as the initial state inactivates the JC interaction in the QRM dynamics
 278 in CRF, seeing that according to the eigenvalue equation (11f), H_{JC} only generates plane wave evolution
 279 $e^{-\frac{i}{\hbar}E_{gn}^-t}|\Psi_{gn}^-\rangle$.

The general time evolving state $|\bar{\Psi}_{CRF}(t)\rangle$ of general QRM dynamics in CRF is generated from the general initial $n \geq 0$ JC eigenstate $|\Psi_{gn}^-\rangle$ through the effective AJC Hamiltonian \bar{H}_{AJC} according to

$$|\bar{\Psi}_{CRF}(t)\rangle = \bar{U}_{AJC}(t)|\Psi_{gn}^-\rangle \quad (12a)$$

where the time evolution operator $\bar{U}_{AJC}(t)$ is defined in equations (10a)-(10b). Substituting $|\Psi_{gn}^-\rangle$ from equation (11h) into equation (12a) gives the form

$$\begin{aligned} |\bar{\Psi}_{CRF}(t)\rangle &= \frac{1}{\sqrt{2(1+c_{gn})}} ((1+c_{gn})|\bar{\Psi}_{gn}(t)\rangle - s_{gn}|\bar{\Psi}_{en-1}(t)\rangle) \\ |\bar{\Psi}_{gn}(t)\rangle &= \bar{U}_{AJC}(t)|\psi_{gn}\rangle ; \quad |\bar{\Psi}_{en-1}(t)\rangle = \bar{U}_{AJC}(t)|\psi_{en-1}\rangle \end{aligned} \quad (12b)$$

Applying the AJC qubit state transition operator \hat{A} from equation (9c) on $|\psi_{gn}\rangle$, $|\psi_{en-1}\rangle$ generates the respective qubit states $(|\psi_{gn}\rangle$, $|\bar{\phi}_{gn}\rangle)$, $(|\psi_{en-1}\rangle$, $|\bar{\phi}_{en-1}\rangle)$ satisfying state transition algebraic operations

$$\begin{aligned} \hat{A}|\psi_{gn}\rangle &= \bar{R}_{en+1}|\bar{\phi}_{gn}\rangle ; \quad \hat{A}|\bar{\phi}_{gn}\rangle = \bar{R}_{gn+1}|\psi_{gn}\rangle ; \quad |\bar{\phi}_{gn}\rangle = -\bar{c}_{gn+1}|\psi_{gn}\rangle + \bar{s}_{gn+1}|\psi_{en+1}\rangle \\ |\psi_{en+1}\rangle &= |en+1\rangle ; \quad \bar{R}_{gn+1} = g\sqrt{(n+1) + (\xi + \varepsilon)^2} ; \quad \bar{c}_{gn+1} = \frac{\bar{\delta}}{2\bar{R}_{gn+1}} ; \quad \bar{s}_{gn+1} = \frac{g\sqrt{n+1}}{\bar{R}_{gn+1}} \end{aligned} \quad (12c)$$

$$\begin{aligned} \hat{A}|\psi_{en-1}\rangle &= \bar{R}_{en-1}|\bar{\phi}_{en-1}\rangle ; \quad \hat{A}|\bar{\phi}_{en-1}\rangle = \bar{R}_{en-1}|\psi_{en-1}\rangle ; \quad |\bar{\phi}_{en-1}\rangle = \bar{c}_{en-1}|\psi_{en-1}\rangle + \bar{s}_{en-1}|\psi_{gn-2}\rangle \\ |\psi_{gn-2}\rangle &= |gn-2\rangle ; \quad \bar{R}_{en-1} = g\sqrt{(n-1) + (\xi + \varepsilon)^2} ; \quad \bar{c}_{en-1} = \frac{\bar{\delta}}{2\bar{R}_{en-1}} ; \quad \bar{s}_{en-1} = \frac{g\sqrt{n-1}}{\bar{R}_{en-1}} \end{aligned} \quad (12d)$$

280 where \bar{R}_{gn+1} , \bar{R}_{en-1} are the respective Rabi frequencies of qubit oscillations.

Substituting $\bar{U}_{AJC}(t)$ from equation (10b) into equation (12b), noting

$$(\hat{N} - 1)|\psi_{gn}\rangle = (n+1)|\psi_{gn}\rangle ; \quad (\hat{N} - 1)|\psi_{en-1}\rangle = (n-1)|\psi_{en-1}\rangle \quad (12e)$$

and expanding $e^{-it\hat{A}}$ in even and odd power terms similar to the corresponding JC time evolution operator expansion in equation (6d), then substituting into equation (12b), we apply \hat{A} on $|\psi_{gn}\rangle$, $|\psi_{en-1}\rangle$ even and odd number times using the qubit state transition algebraic operations from equations (12c), (12d) giving relations similar to equation (5g) and introduce trigonometric functions in the expansions as appropriate to obtain

$$\begin{aligned} |\bar{\Psi}_{gn}(t)\rangle &= e^{-i\omega(n+1)t}(\cos(\bar{R}_{gn+1}t)|\psi_{gn}\rangle - i\sin(\bar{R}_{gn+1}t)|\bar{\phi}_{gn}\rangle) \\ |\bar{\Psi}_{en-1}(t)\rangle &= e^{-i\omega(n-1)t}(\cos(\bar{R}_{en-1}t)|\psi_{en-1}\rangle - i\sin(\bar{R}_{en-1}t)|\bar{\phi}_{en-1}\rangle) \end{aligned} \quad (12f)$$

Substituting these into equation (12b) provides the explicit form of the general time evolving QRM state $|\bar{\Psi}_{CRF}(t)\rangle$ in CRF generated by the effective AJC Hamiltonian \bar{H}_{AJC} from the general $n \geq 0$ initial entangled JC eigenstate $|\Psi_{gn}^-\rangle$. Introducing the definitions of the states ($|\psi_{gn}\rangle$, $|\psi_{en+1}\rangle$, $|\bar{\phi}_{gn}\rangle$) and ($|\psi_{en-1}\rangle$, $|\psi_{gn-2}\rangle$, $|\bar{\phi}_{en-1}\rangle$) from equations (11a), (12c), (12d) reveals that the general time evolving QRM state $|\bar{\Psi}_{CRF}(t)\rangle$ in CRF is a time evolving entangled state.

We easily obtain orthonormalization relations

$$\begin{aligned} \langle \bar{\Psi}_{gn}(t) | \bar{\Psi}_{gn}(t) \rangle &= 1 ; \quad \langle \bar{\Psi}_{gn}(t) | \bar{\Psi}_{en-1}(t) \rangle = 0 ; \quad \langle \bar{\Psi}_{en-1}(t) | \bar{\Psi}_{gn}(t) \rangle = 0 ; \quad \langle \bar{\Psi}_{en-1}(t) | \bar{\Psi}_{en-1}(t) \rangle = 1 \\ \langle \bar{\Psi}_{CRF}(t) | \bar{\Psi}_{CRF}(t) \rangle &= 1 \end{aligned} \quad (12g)$$

We obtain the AJC excitation number $\bar{N}(t)$ in the general time evolving QRM state $|\bar{\Psi}_{CRF}(t)\rangle$ in the form

$$\bar{N}(t) = n + 2 - \frac{s_{gn}^2}{1 + c_{gn}} \quad (12h)$$

which once again confirms that the AJC excitation number is conserved in CRF as expected according to the commutation relation $[\hat{N}, \bar{H}_{AJC}] = 0$ in equation (4a). The atomic population inversion and antinormal order excitation $\bar{s}_z(t)$, $\bar{s}_- \bar{s}_+(t)$, the field mode mean antinormal order photon number $\bar{a}\bar{a}^*(t)$ and the JC excitation number $\bar{N}(t)$ (normal order) in the QRM state $|\bar{\Psi}_{CRF}(t)\rangle$ are obtained in the form

$$\begin{aligned} \bar{s}_z(t) &= -\frac{1}{4(1+c_{gn})} \{ (1+c_{gn})^2(1-2\bar{s}_{gn+1}^2 \sin^2(\bar{R}_{gn+1}t)) - s_{gn}^2(1-2\bar{s}_{en-1}^2 \sin^2(\bar{R}_{en-1}t)) \} \\ \bar{s}_- \bar{s}_+(t) &= \frac{1}{2} - \bar{s}_z(t) ; \quad \bar{a}\bar{a}^*(t) = n + \frac{3}{2} - \frac{s_{gn}^2}{1+c_{gn}} + \bar{s}_z(t) ; \quad \bar{N}(t) = n + 1 - \frac{s_{gn}^2}{1+c_{gn}} + 2\bar{s}_z(t) \end{aligned} \quad (12i)$$

We observe that setting $n = 0$ reduces $|\bar{\Psi}_{CRF}(t)\rangle$ in equation (12b) to $|\Psi_{g0}(t)\rangle$ in equation (10d), (10e) and the results in equation ((12i) reduce to the corresponding results in equation (10g), showing that QRM dynamical evolution from the general $n \geq 0$ entangled JC eigenstate $|\Psi_{gn}^-\rangle$ in equation (11h) is a consistent generalization of the dynamical evolution from the $n = 0$ JC eigenstate $|\psi_{g0}\rangle$ in equation (9a). Plots of the mean values in equation (12i) for $n = 0$ reproduce the corresponding plots in Fig.8-Fig.11, while plots for field mode initial photon numbers $n \geq 1$ show time evolution characterized by quantum collapses and revivals largely determined by the initial field mode photon number n .

We have plotted the atomic antinormal excitation number $X = \bar{s}_- \bar{s}_+(t)$, field mode mean antinormal photon number $F = \bar{a}\bar{a}^*(t)$ and the JC excitation number $\bar{N}(t)$ for arbitrarily chosen initial photon number $n = 40$ and dimensionless parameters ξ , ε , in Fig.12, Fig.13, Fig.14, respectively, which clearly undergo collapses and revivals similar to the corresponding JC cases in RF presented in Fig.5-Fig.7. Again, we observe that the field mode mean photon number collapse-revival profile takes the form obtained in the full QRM DSC regime in [1]. Here again, we consider the collapse-revival phenomenon to be a dynamical feature of AJC interaction mechanism for atom-field initial superposition state such as the $n \geq 0$ entangled JC eigenstate, noting that CRF where the effective AJC interaction is dominant is not necessarily equivalent to the USC-DSC regime of QRM as usually defined.

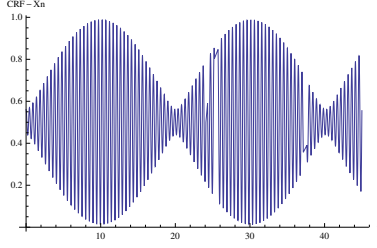


Figure 12: AJC-atomic antinormal excitation number in CRF $\overline{s_- s_+}(\tau)$, $\tau = gt$: $\xi = \frac{1}{1.31}$; $\varepsilon = 0.16$; $n = 40$

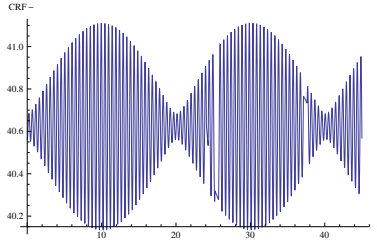


Figure 13: AJC-field mode mean antinormal photon number in CRF $\overline{aa^*}(\tau)$, $\tau = gt$: $\xi = \frac{1}{1.31}$; $\varepsilon = 0.16$; $n = 40$

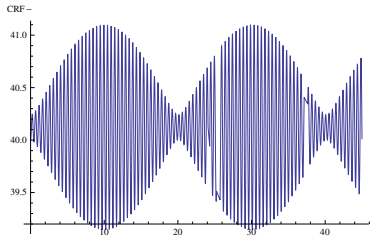


Figure 14: JC-excitation number in CRF $\overline{N}(\tau)$, $\tau = gt$: $\xi = \frac{1}{1.31}$; $\varepsilon = 0.16$; $n = 40$

4 Conclusion

By demonstrating that the AJC interaction has a conserved excitation number operator and is exactly solvable, we have addressed a major challenge of theoretical and experimental efforts to investigate the internal dynamics of QRM. We have established that QRM has two correlated dynamical frames; the rotating frame (RF) where the dynamics is dominated by the exactly solved JC interaction characterized by red-sideband transitions, with a conserved JC excitation number operator which generates the $U(1)$ symmetry of RF, and, the counter-rotating frame (CRF) where the dynamics is dominated by the exactly solved AJC interaction characterized by blue-sideband transitions, with a conserved AJC excitation number operator which generates the $U(1)$ symmetry of CRF. The two conserved, JC and AJC, excitation number operators commute and generate a common parity symmetry operator of both JC and AJC interactions, thereby providing the parity symmetry operator of the full QRM. The $U(1)$ symmetry operator of JC reduces QRM Hamiltonian to an effective JC Hamiltonian in an RWA in RF, while the $U(1)$ symmetry operator of AJC reduces QRM Hamiltonian to an effective AJC Hamiltonian in a CRWA in CRF. Considering the initial atom-field states $|e0\rangle$ and $|g0\rangle$, preferred as the fundamental QRM initial states in the experiments, we have established that the effective JC Hamiltonian H_{JC} generates dynamical evolution of the state $|e0\rangle$ into a time evolving entangled state in RF, while the effective AJC Hamiltonian \bar{H}_{AJC} generates dynamical evolution of the (absolute) ground state $|g0\rangle$ into a time evolving entangled state in CRF, thus addressing another major challenge of determining QRM dynamics beyond RWA. Identifying the initial atom-field states $|e0\rangle$ and $|g0\rangle$ as eigenstates of the effective AJC and JC Hamiltonians, respectively, we have derived the corresponding general $n \geq 0$ entangled AJC and JC eigenstates as consistent generalizations of QRM initial states in RF under RWA and CRF under CRWA. The general QRM state in RF or CRF is then a general time evolving entangled state generated by H_{JC} from the general $n \geq 0$ initial entangled AJC eigenstate $|\bar{\Psi}_{en}^+\rangle$ or a general time evolving entangled state generated by \bar{H}_{AJC} from the general $n \geq 0$ initial entangled JC eigenstate $|\Psi_{gn}^-\rangle$. In QRM dynamics from the general $n \geq 0$ initial entangled states in RF or CRF, the general time evolution of the atomic population inversion and excitation number, the field mode mean photon number and the JC/AJC excitation numbers undergo quantum collapses and revivals determined by the initial field mode photon numbers $n \geq 1$, where we note that the JC excitation number is conserved in RF, but evolves in time in CRF, while the AJC excitation number is conserved in CRF, but evolves in time in RF. An important point which arises is that the clear specification of the QRM dynamical frames RF and CRF dominated by the exactly solved effective JC and AJC interaction mechanisms, respectively, now calls to question the true physical interpretation of the coupling regimes, which have been characterized in the theoretical models and experimental designs as the weak-strong coupling (WSC) regime where JC interaction dominates and the USC-DSC regime where AJC interaction is believed to be dominant. Considering the QRM dynamical frames as we have specified and demonstrated their physical characteristics in the present article, can we consistently interpret the WSC regime as RF dominated by the JC interaction mechanism and the USC-DSC regime as CRF dominated by the AJC interaction mechanism? Such an interpretation may have to be reviewed, noting that the basic definitions of RF/CRF do not depend explicitly on the dimensionless coupling parameter $\frac{g}{\omega}$ used to characterize the coupling regimes WSC, USC-DSC and that the respective JC and AJC qubit state transition algebraic operations in equations (5e-5f, 8c-8d) which characterize dynamics in RF and (9d-9e, 12c-12d) which characterize dynamics in CRF are generally applicable over the physical parameter ranges, independently of the coupling regimes. We may therefore interpret USC-DSC simply as the coupling regime where neither RWA nor CRWA applies and the general QRM dynamics must then be determined by the full QRM Hamiltonian $H_R \sim \frac{1}{2}(H_{JC} + \bar{H}_{AJC})$. In this respect, we may take advantage of the useful property that each component Hamiltonian H_{JC} , \bar{H}_{AJC} generates exact dynamical evolution to develop algebraic methods to disentangle the full QRM time evolution operator $U_{QRM}(t) \sim e^{-\frac{it}{2\hbar}(H_{JC} + \bar{H}_{AJC})}$ to determine the general dynamics generated by the full QRM Hamiltonian H_R .

5 Acknowledgement

I thank Maseno University for providing facilities and a conducive work environment during the preparation of the manuscript.

References

- 351
- 352 [1] F A Wolf, F Vallone, et al, 2013 Dynamical correlation functions and the quantum Rabi model,
353 Phys.Rev. **A 87**, 023835
- 354 [2] J Casanova, G Romero, et al, 2010 Deep strong coupling regime of the Jaynes-Cummings model,
355 Phys.Rev.Lett. **105**, 263603
- 356 [3] D Braak, 2011 On the integrability of the Rabi model, Phys.Rev.Lett. **107**, 100401
- 357 [4] D Z Rossatto, C J Villas-Boas, M Sanz, E Solano, 2017 Spectral characterization of coupling regimes in
358 the quantum Rabi model, Phys.Rev. **A 96**, 013849
- 359 [5] Z Li, D Ferri, M T Batchelor, 2021 Nonorthogonal-qubit-state expansion for the asymmetric quantum
360 Rabi model, Phys.Rev. **A 103**, 013711
- 361 [6] J A Omolo 2017 Conserved excitation number and $U(1)$ -symmetry operators for the anti-
362 rotating (anti-Jaynes-Cummings) term of the Rabi Hamiltonian, Preprint-ResearchGate,
363 DOI:10.13140/RG.2.2.30936.80647 ; arXiv: 2103.06577 [quant-ph]
- 364 [7] J A Omolo 2018 Polariton and anti-polariton qubits in the Rabi model, Preprint-ResearchGate,
365 DOI:10.13140/RG.2.2.11833.67683
- 366 [8] J A Omolo 2019 Photospins in the quantum Rabi model, Preprint-ResearchGate,
367 DOI:10.13140/RG.2.2.27331.96807
- 368 [9] D Lv, S An, et al, 2018 Quantum simulation of the quantum Rabi model in a trapped ion, Phys.Rev. **X**
369 **8**, 021027
- 370 [10] N K Longford, R Sagastizabal, et al, 2017 Experimentally simulating the dynamics of quantum light
371 and matter at deep-strong coupling, Nat.Comm. **8**, 1715
- 372 [11] S Felicetti, G Romero, E Solano, C Sabin 2017 Quantum Rabi model in a superfluid Bose-Einstein
373 condensate, Phys.Rev. **A 96**, 033839
- 374 [12] Y H Chen, W Qin, X Wang, A Miranowicz, F Nori 2021 Shortcuts to adiabaticity for the quan-
375 tum Rabi model : efficient generation og giant entangled cat states via parametric amplification,
376 Phys.Rev.Lett. **126**, 023602
- 377 [13] J Le Boite 2020 Theoretical methods for ultrastrong light-matter coupling, arXiv: 2001.08715 [quant-ph]
- 378 [14] P Forn-Diaz, L Lamata, E Rico, J Kono, E Solano 2019 Ultrastrong coupling regimes of light-matter
379 interactions, Rev.Mod.Phys. **91**, 025005
- 380 [15] A F Kockum, A Miranowicz, S De Liberato, S Savasta, F Nori 2019 Ultrastrong coupling between light
381 and matter, Nat.Rev.Phys. **1**, 19

Figures

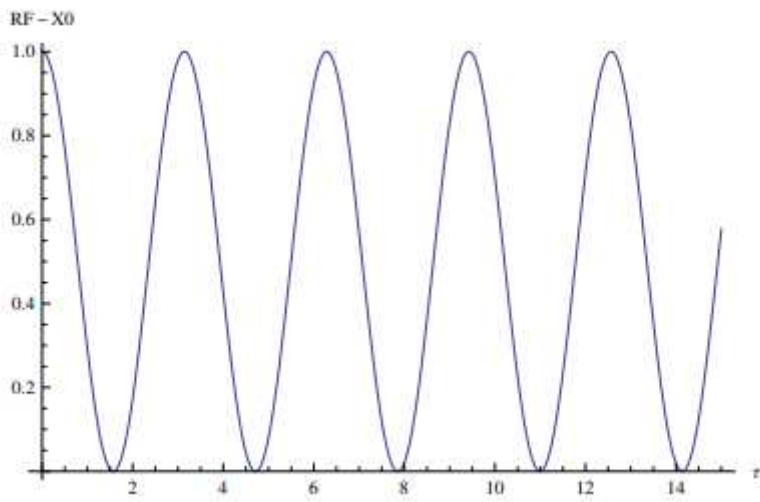


Figure 1

JC-atomic excitation number in RF $s+s-(\tau)$, $\tau = gt$; $\xi = 0$; $\varepsilon = \dots$

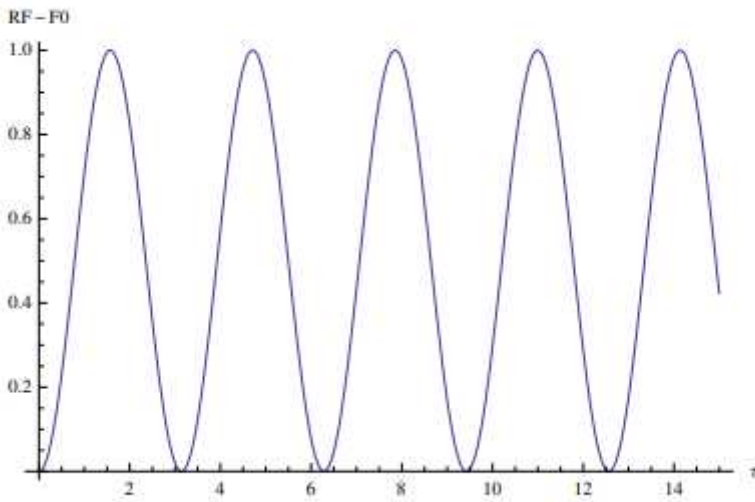


Figure 2

Please see the manuscript file to view this figure caption.

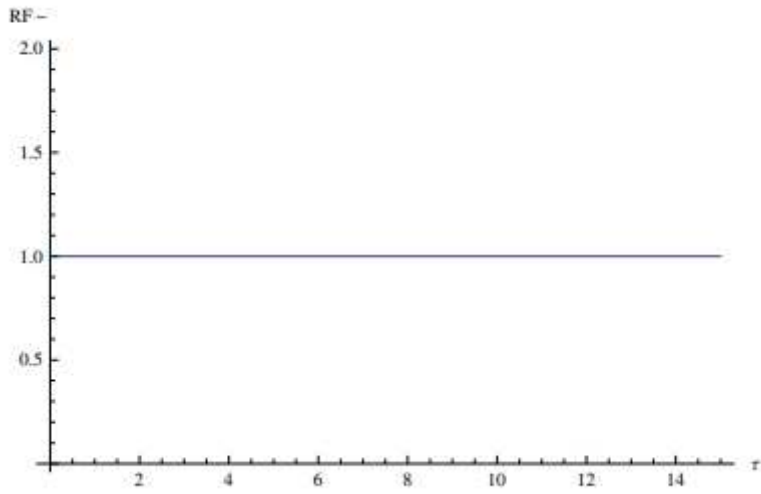


Figure 3

Please see the manuscript file to view this figure caption.

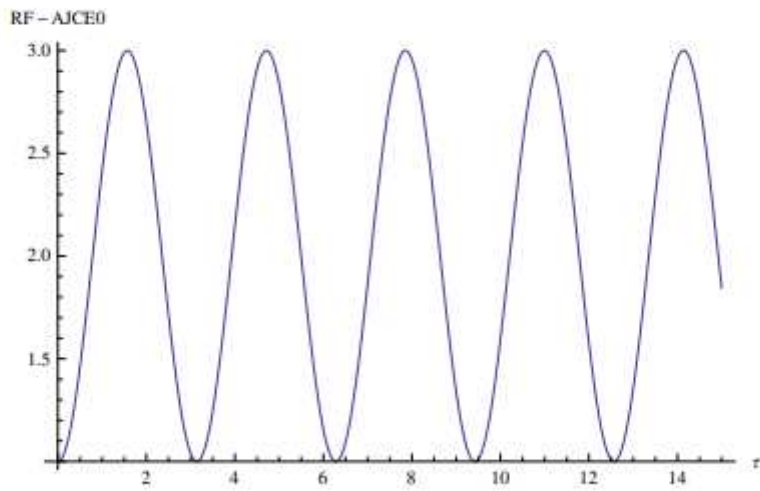


Figure 4

Please see the manuscript file to view this figure caption.

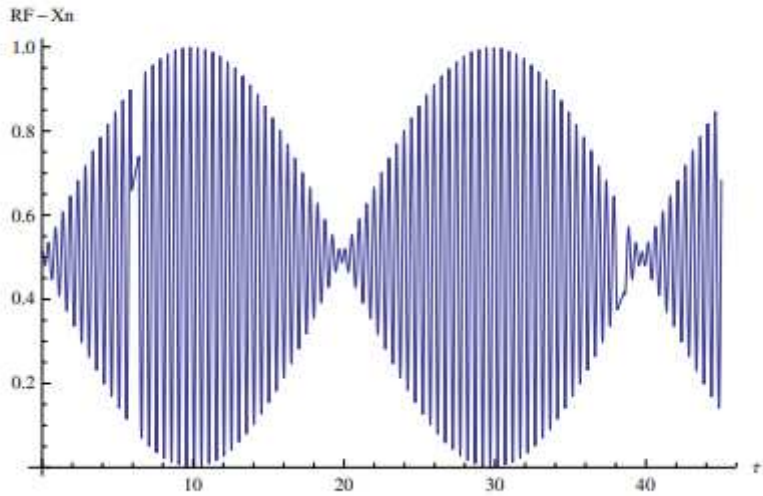


Figure 5

Please see the manuscript file to view this figure caption.

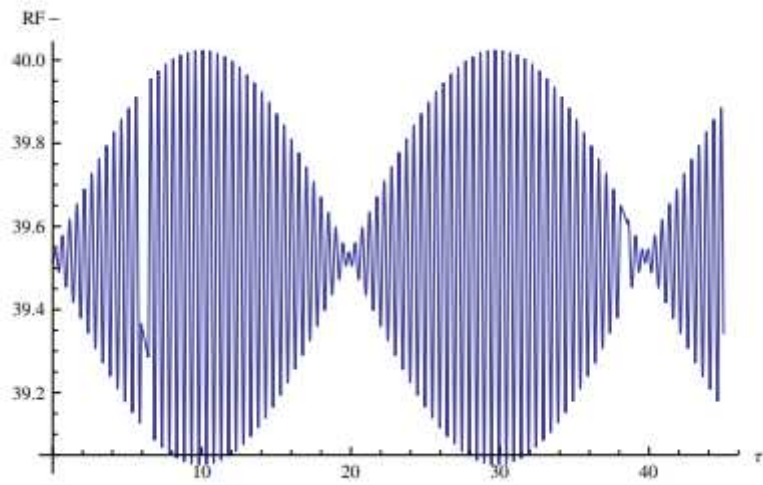


Figure 6

Please see the manuscript file to view this figure caption.

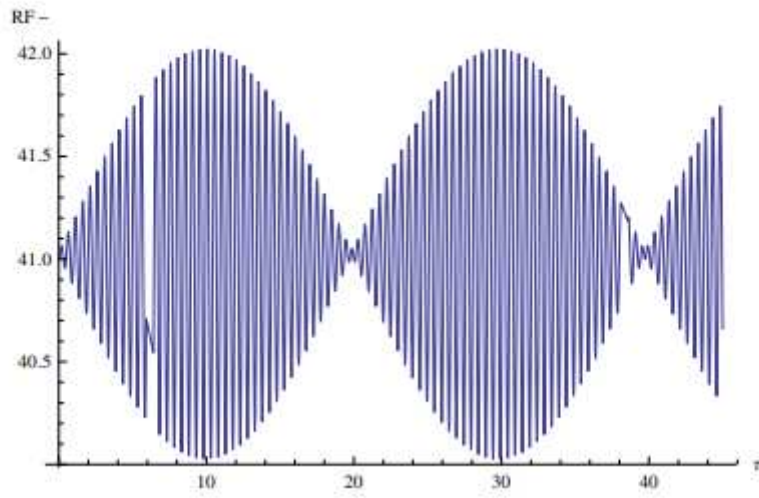


Figure 7

Please see the manuscript file to view this figure caption.

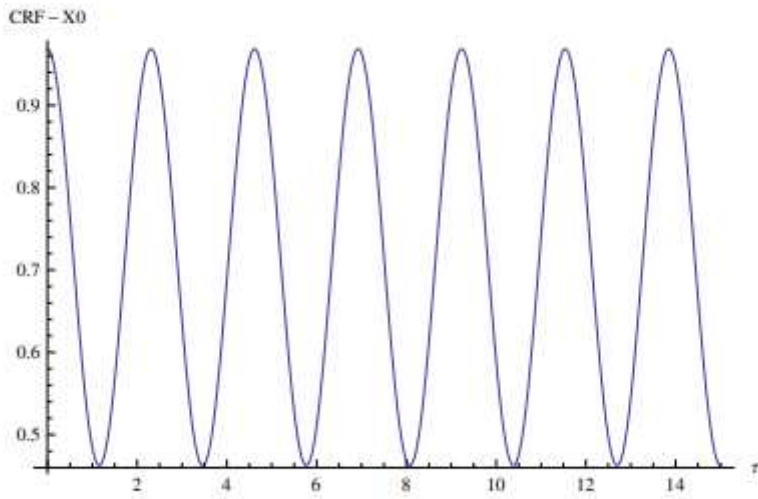


Figure 8

Please see the manuscript file to view this figure caption.

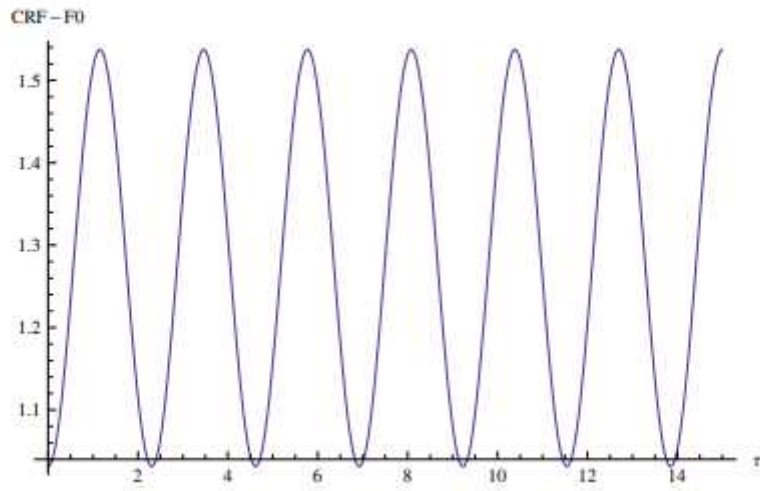


Figure 9

Please see the manuscript file to view this figure caption.

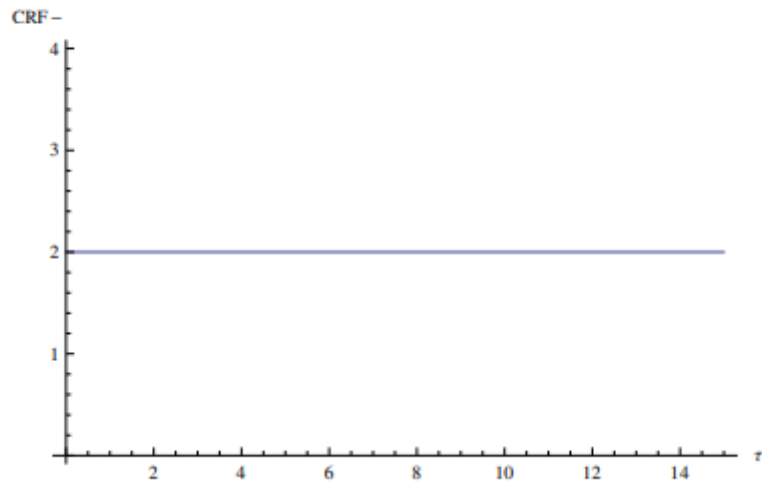


Figure 10

Please see the manuscript file to view this figure caption.

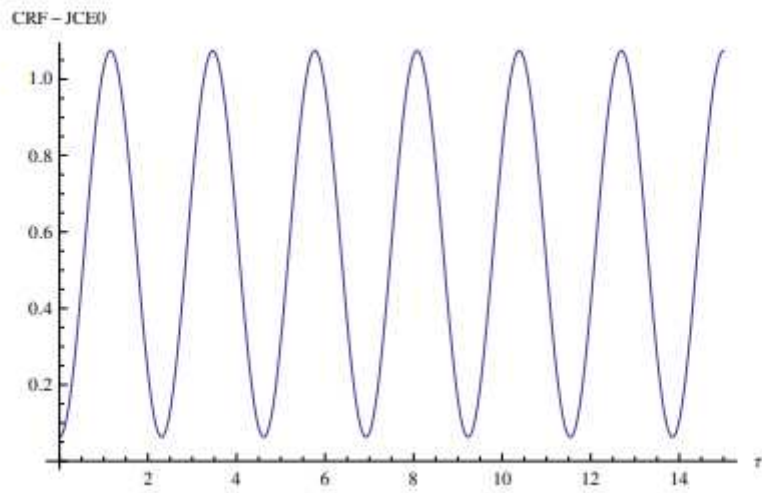


Figure 11

Please see the manuscript file to view this figure caption.

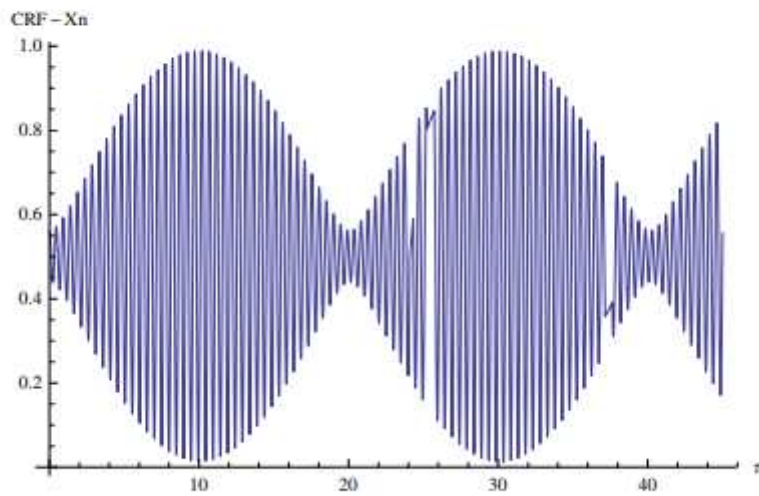


Figure 12

Please see the manuscript file to view this figure caption.

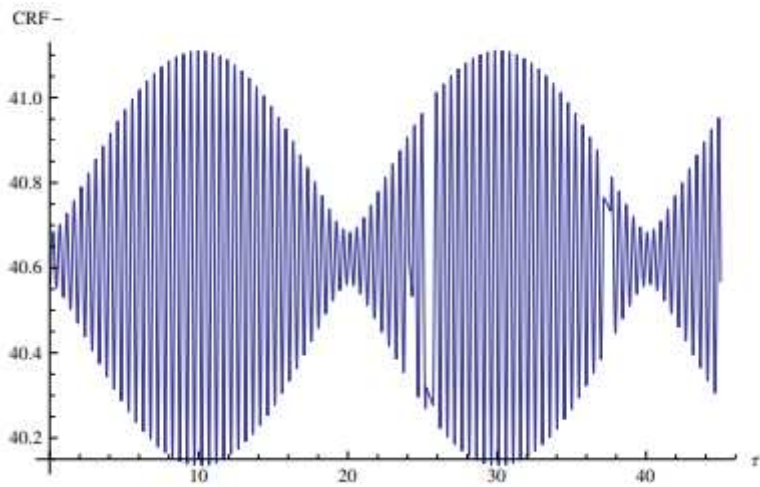


Figure 13

Please see the manuscript file to view this figure caption.

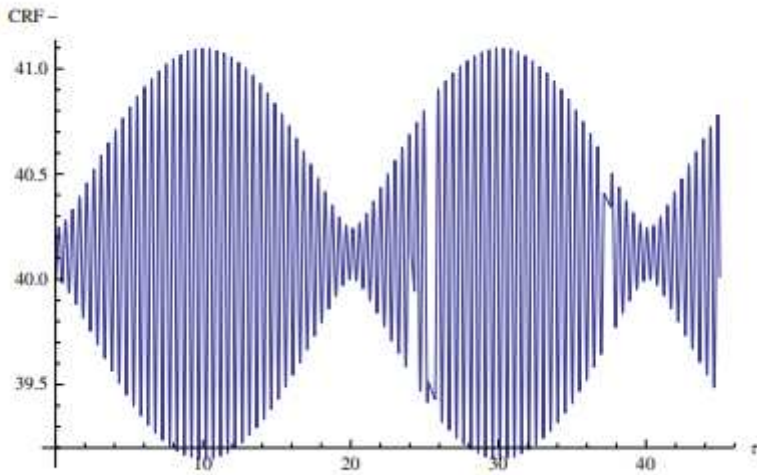


Figure 14

Please see the manuscript file to view this figure caption.